AFOSR-TR- 84-0255

14

Copy No. 4

MRC-R-825

FINAL REPORT:

IONOSPHERIC GRAVITY WAVES FROM NUCLEAR SURFACE BURSTS

ARPA ORDER:	4397
PROGRAM CODE:	3D60
CONTRACTOR:	MISSION RESEARCH CORPORATION
EFFECTIVE CONTRACT DATE:	15 NOVEMBER 1982
CONTRACT EXPIRATION DATE:	31 JANUARY 1984
AMOUNT OF CONTRACT:	$148,690
CONTRACT NUMBER:	F49620-83-C-0034
PRINCIPAL INVESTIGATOR:	GARY MCCARTOR (805) 963-8761

Sponsored by
Advanced Research Projects Agency (DOD)
ARPA Order No. 4397
Monitored by AFOSR Under Contract # F49620-83-C-0034

The views and conclusions contained in this document are those of the authors and should not be interpreted as necessarily representing the official policies, either expressed or implied, of the Defense Advanced Research Projects Agency or the U.S. Government.

Approved for public release;
distribution unlimited.

UNCLASSIFIED

AD-A140585

SECURITY CLASSIFICATION OF THIS PAGE (When Data Entered)

REPORT DOCUMENTATION PAGE	READ INSTRUCTIONS BEFORE COMPLETING FORM
1. REPORT NUMBER AFOSR-TR- 84-0255 2. GOVT ACCESSION NO.	3. RECIPIENT'S CATALOG NUMBER
4. TITLE (and Subtitle) IONOSPHERIC GRAVITY WAVES FROM NUCLEAR SURFACE BURSTS	5. TYPE OF REPORT & PERIOD COVERED FINAL REPORT 14 Nov 83 - 31 Jan 84
	6. PERFORMING ORG. REPORT NUMBER MRC-R-825
7. AUTHOR(s) R. GOLDFLAM G. MCCARTOR B. WORTMAN	8. CONTRACT OR GRANT NUMBER(s) F-49620-83-C-0034
9. PERFORMING ORGANIZATION NAME AND ADDRESS MISSION RESEARCH CORPORATION 735 State State St., PO Drawer 719 Santa Barbara, CA 93101	10. PROGRAM ELEMENT, PROJECT, TASK AREA & WORK UNIT NUMBERS 61102F 2309/A1
11. CONTROLLING OFFICE NAME AND ADDRESS Defense Advanced Projects Agency 1400 Wilson Blvd. Arlington, VA 27709	12. REPORT DATE March 15, 1984
	13. NUMBER OF PAGES 63
14. MONITORING AGENCY NAME & ADDRESS(if different from Controlling Office) Air Force Office of Scientific Research Bolling Air Force Base Washington, DC 20332	15. SECURITY CLASS (of this report) UNCLASSIFIED
	15a. DECLASSIFICATION/DOWNGRADING SCHEDULE

16. DISTRIBUTION STATEMENT (of this Report)

Approved for public release, Distribution unlimited.

17. DISTRIBUTION STATEMENT (of the abstract entered in Block 20, if different from Report)

18. SUPPLEMENTARY NOTES

19. KEY WORDS (Continue on reverse side if necessary and identify by block number)

Gravity Waves
Nuclear Test Detection
Blast Wave
Rising Fireball

20. ABSTRACT (Continue on reverse side if necessary and identify by block number)

The rising fireball and the blast wave are investigated as possible sources of atmospheric gravity waves in a stratified medium (isothermal atmosphere) using previously developed methods. Exact and approximate calculations are carried out and the results are compared with observations. We conclude that the blast wave is the predominant source of large amplitude gravity waves.

DD FORM 1 JAN 73 1473 EDITION OF 1 NOV 65 IS OBSOLETE

UNCLASSIFIED

SECURITY CLASSIFICATION OF THIS PAGE (When Data Entered)

AIR FORCE OFFICE OF SCIENTIFIC RESEARCH (AFSC)
NOTICE OF TRANSMITTAL TO DTIC
This technical report has been reviewed and is approved for public release IAW AFR 190-12.
Distribution is unlimited.
MATTHEW J. KERPER
Chief, Technical Information Division

TABLE OF CONTENTS

LIST OF ILLUSTRATIONS

SECTION 1
INTRODUCTION

Ionospheric disturbances have been observed following large, low-altitude nuclear weapons tests conducted by the U.S.A. in 1962[1-2], the Soviet Union in 1961[3] and France in 1967[4]. Close inspection of the data reveals that there appear to be two types of waves: a wave which propagates to at least several thousand kilometers from the burst and whose period depends on the observation point; a wave which propagates all the way around the earth (possibly more than once) and whose period is around 15 minutes. There was agreement very soon after the observations were made that the ionospheric disturbances were due to a system of acoustic gravity waves set up by the explosion.

The ionospheric observations inspired a substantial research program on the subject of acoustic gravity waves[5]. During this effort much was learned about the rather unusual features of the propagation of such waves. Of particular importance was the classification[6] of the waves as either freely propagating (which can exist in any stratified atmosphere) or ducted (which can exist only in an atmosphere with a certain type of temperature structure); the earth's atmosphere is such as to support both freely propagating and ducted types of waves.

In spite of the progress made in understanding acoustic gravity waves the fundamental issues associated with the test data were never resolved. In particular it was never determined what aspect of the explosion is responsible for creating the gravity waves or what type of wave (ducted or freely propagating) was most important for producing the ionospheric disturbances. The most commonly suggested source mechanisms were the blast wave and motions associated with the rising fireball.[3,9] More

recently we have suggested that the heated region above 100 km altitude which is created directly over a low altitude explosion by the restrengthening of the blast wave might act as a source of acoustic gravity waves.[7]

In 1982 DARPA/AFOSR tasked MRC to use mathematical procedures developed at MRC during the 1970's to perform calculations to determine what the most important source or sources for the nuclear-explosion-induced gravity waves are. This document is the final report on that effort. We have made calculations for the coupling of the blast wave, the rising fireball and the high altitude hot spot to both ducted and freely propagating acoustic gravity waves. Although the simplified nature of our atmospheric models precludes detailed comparisons between the calculations and the data, we can compare the general features of the two. The results allow us to draw these conclusions: 1) the major source of the large amplitude ionospheric gravity wave observed following the U.S. and Russian tests (the wave with periods ranging from 30 minutes to more than two hours) is the blast wave and the energy is transmitted by the freely propagating modes; 2) the source of the ~15 minute period waves that were observed to go all the way around the world is the high altitude hot spot and the energy is traveling in the ducted modes; 3) the motions associated with the rising fireball give a smaller signal in the freely propagating modes than the blast wave and a smaller signal in the ducted modes than the high altitude hot spot; 4) it appears that ionospheric observations will be of limited use in detecting small (<10kT) low altitude detonations at large distances (>1000km) from the burst.

In the next section of the present report we briefly review the mathematical procedures developed in References 6 and 7; we then formulate, within the context of these procedures, the problem of the coupling of the blast wave to the freely propagating acoustic gravity waves in an isothermal atmosphere. The solution is given as a sum of integrals which represent, in our way of thinking about the problem, a sum over

eigenstates. We have evaluated these integrals numerically and the results are presented. The fact that our current calculations are for an isothermal atmosphere whereas the data are for a region of the real atmosphere over which the temperature varies considerably causes certain ambiguities in comparing our results with data; the way we have resolved these ambiguities is described in detail in Section 2C. The results of the comparison of the calculations with the data shows good agreement for both the amplitude of the disturbance and its wave form; this is the first calculation of the acoustic gravity wave generated by a nuclear explosion to show such good agreement. We would expect the agreement between the calculations and the data to be improved by the use of more realistic atmospheric models (such calculations would also substantially reduce the ambiguities mentioned above) but the agreement is already sufficiently good that we are confident that the blast wave is the source mechanism for the large amplitude, varying frequency gravity waves.

Prior to resorting to numerical procedures for evaluation the integrals we attempted to estimate them in the stationary phase approximation. This procedure worked well enough for sufficiently late time but the stationary phase approximation proved surprisingly ineffective for times during the first several oscillations after the arrival of the signal (the interesting times for our work). In Section 2 and Appendix A we give the details of our stationary phase calculations and the difficulties encountered. We also remark on the relevance of the results to the previous work of other workers.[4]

In Section 3 we consider the coupling of the motions associated with the rising fireball to acoustic gravity waves. The calculations are done with relatively simple models consisting of point sources; the calculations are done in the approximation that only low frequencies contribute. The reason that these calculations have been done in less detail than those for the blast wave is that the calculations with the simple

model make it clear that the motions associated with the rising fireball are a much weaker source of gravity waves than the blast wave.

In Reference 7 we presented calculations which gave the coupling of the high altitude hot spot to ducted gravity modes. In that report we gave specific calculations only for small events; the formulas given there can be applied to larger events so as to allow comparison with the data in Reference 4. The comparison between the calculation and the data shows good agreement for the amplitude but somewhat less good agreement for the wave form. We believe the differences between the calculated waveform and the observed one are due to the effects of dispersion which is absent from our calculations but present to some extent in the real atmosphere. Although we expect the dispersion to be small, for the ten thousand kilometer path lengths of the observations the waveform could have become appreciably distorted.

By combining the calculations presented in this report with those presented in Reference 7 we arrive at the conclusions stated above.

SECTION 2
GRAVITY WAVES GENERATED BY THE BLAST WAVE*

A. INTRODUCTION

In this section we investigate the gravity wave response of the atmosphere to a low altitude nuclear burst using methods developed earlier in References 6 and 7. Our goal in this section is to determine the gravity wave signal generated by the blast wave and carried by the freely propagating modes and to compare with limited experimental observations[1-5] This investigation is complicated by the fact that the Euler-Lagrange equations for a stratified atmosphere are nonlinear. These nonlinearities cause lengthening and strengthening of the initial blast wave during the early time development (to about 100 km from the point of blast) which continues until the relative overpressure is about 5 percent. This early time development has been described by a model in Reference 8. For large distances, say 1000 km or more, the relative pressure variation is sufficiently small and we can assume that the hydrodynamics is well described by linearized Euler-Lagrange equations in an isothermal atmosphere. To obtain a smooth transition from the nonlinear regime to the linearized one, we use the calculations of amplitude A and pulse length L of Reference 8 to define the initial boundary condition at some chosen height D for the linearized differential equations for the atmosphere. From this point on the linearized equations are solved numerically using methods of References 6 and 7 and these results are compared to observations and the stationary phase approximation, an approximation commonly used in estimating gravity wave response. As we shall see the exact calculation compare favorably with available observations and in passing

* The methods used in this report were developed and presented in Reference 7. For completeness, we review the methods in this Section; much of this material is taken from Reference 7.

we shall note that the stationary approximation is very inaccurate in estimating the amplitude of the gravity waves arising from a blast wave.

B. HYDRODYNAMIC VARIABLES AND EQUATIONS

To begin with, we consider the case of one isothermal layer. The hydrostatic solution about which we wish to perturb is given by

$$\vec{u} = 0$$
$$P = P_o e^{-z/H}$$
$$\rho = \rho_o e^{-z/H}$$

where $\vec{u}$ is the fluid velocity, P the pressure, and ρ the density. P_o, ρ_o, and H are constant related by $P_o = \rho_o H g$, where g is the acceleration of gravity. We define perturbing variable by the relations

$$\vec{u} = \tilde{\vec{V}} e^{z/2H}$$
$$P = e^{-z/H}(P_o + \tilde{P} e^{z/2H})$$
$$\rho = e^{-z/H}(\rho_o + \tilde{\rho} e^{z/2H}).$$

We have chosen the exponential factors so that the perturbing functions $\tilde{V}$, $\tilde{P}$, $\tilde{\rho}$ will be bounded for all values of x,y,z, and t, and, for compact disturbances, will be square integrable functions of x,y, and z for any value of t. (This fact is not obvious but is seen in the results below.) For these variables the linearized hydrodynamic equations take on the familiar form

$$\frac{\partial \tilde{V}_z}{\partial t} = \frac{1}{2H\rho_o}\tilde{P} - \frac{1}{\rho_o}\frac{\partial \tilde{P}}{\partial z} - \frac{g}{\rho_o}\tilde{\rho}$$

$$\frac{\partial \tilde{P}}{\partial t} = -\gamma P_o \frac{\partial \tilde{V}_x}{\partial x} - \gamma P_o \frac{\partial \tilde{V}_z}{\partial z} - \left(\frac{\gamma}{2} - 1\right)\frac{P_o}{H}\tilde{V}_z - \gamma P_o \frac{\partial \tilde{V}_y}{\partial y}$$

$$\frac{\partial \tilde{V}_x}{\partial t} = -\frac{1}{\rho_o}\frac{\partial \tilde{P}}{\partial x}$$

$$\frac{\partial \tilde{V}_y}{\partial t} = -\frac{1}{\rho_o}\frac{\partial \tilde{P}}{\partial y}$$

$$\frac{\partial \tilde{\rho}}{\partial t} = \frac{\rho_o}{2H}\tilde{V}_z - \rho_o \frac{\partial \tilde{V}_x}{\partial x} - \rho_o \frac{\partial \tilde{V}_z}{\partial z} - \rho_o \frac{\partial \tilde{V}_y}{\partial y} \qquad (2\text{-}1)$$

We assume a time dependence $e^{-i\omega t}$ for each of the variables and obtain[7]

$$\frac{i}{2H\rho_o}\tilde{P} - \frac{i}{\rho_o}\frac{\partial \tilde{P}}{\partial z} - \frac{ig}{\rho_o}\rho = \omega \tilde{V}_z$$

$$-i\gamma P_o \frac{\partial \tilde{V}_x}{\partial x} - iP_o \frac{\partial \tilde{V}_z}{\partial z} - i\left(\frac{\gamma}{2} - 1\right)\frac{P_o}{H}\tilde{V}_z - i\gamma P_o \frac{\partial \tilde{V}_y}{\partial y} = \omega \tilde{P}$$

$$\frac{-i}{\rho_o}\frac{\partial \tilde{P}}{\partial x} = \omega \tilde{V}_x$$

$$\frac{-i}{\rho_o}\frac{\partial \tilde{P}}{\partial y} = \omega \tilde{V}_y$$

$$\frac{i\rho_o}{2H}\tilde{V}_z - i\rho_o \frac{\partial \tilde{V}_x}{\partial x} - i\rho_o \frac{\partial \tilde{V}_z}{\partial z} - i\rho_o \frac{\partial \tilde{V}_y}{\partial y} = \omega\tilde{\rho} \qquad (2\text{-}2)$$

We now wish to construct a Hilbert space in which our solution will lie. We arrange the functions into a column vector in the order

$$|a\rangle = \begin{pmatrix} \tilde{p} \\ \tilde{V}_z \\ \tilde{V}_x \\ \tilde{V}_y \\ \tilde{\rho} \end{pmatrix}$$

and define the inner product

$$\langle a|b\rangle = \int_{-\infty}^{\infty} \tilde{p}_a^* \tilde{p}_b + \tilde{V}_{za}^* \tilde{V}_{zb} + \tilde{V}_{xa}^* \tilde{V}_{xb} + \tilde{V}_{ya}^* \tilde{V}_{yb} + \tilde{\rho}_a^* \tilde{\rho}_b \; dxdydz \quad (2\text{-}3)$$

Equation 2 takes on the form

$$M|a\rangle = \omega|a\rangle, \quad (2\text{-}4)$$

where the operator M is given by

$$M = \begin{pmatrix} 0 & i\gamma P_o \frac{\partial}{\partial z} - i\left(\frac{\gamma}{2} - 1\right)\frac{P_o}{H} & -i\gamma P_o & -i\gamma P_o & 0 \\ -\frac{i}{\rho_o}\frac{\partial}{\partial z} + \frac{i}{2H\rho_o} & 0 & 0 & 0 & -\frac{ig}{\rho_o} \\ -\frac{i}{\rho_o}\frac{\partial}{\partial x} & 0 & 0 & 0 & 0 \\ -\frac{i}{\rho_o}\frac{\partial}{\partial y} & 0 & 0 & 0 & 0 \\ 0 & -i\rho_o\frac{\partial}{\partial z} + \frac{i\rho_o}{2H} & -i\rho_o\frac{\partial}{\partial x} & -i\rho_o\frac{\partial}{\partial y} & 0 \end{pmatrix} \quad (2\text{-}5)$$

This operator is not symmetric. We define a new vector space

$$a = \begin{pmatrix} a_1 \\ a_2 \\ a_3 \\ a_4 \\ a_5 \end{pmatrix}$$

where

$$a_1 = \frac{\tilde{p}}{\sqrt{\gamma} p_0}$$

$$a_2 = \frac{\sqrt{\gamma}\tilde{v}_z}{c}$$

$$a_3 = \frac{\sqrt{\gamma}\tilde{v}_x}{c} \qquad (c=\sqrt{\gamma g H})$$

$$a_4 = \frac{\sqrt{\gamma}\tilde{v}_y}{c}$$

$$a_5 = \frac{1}{\sqrt{\gamma(\gamma-1)}} \left(\frac{\tilde{p}}{p_0} - \gamma \frac{\tilde{\rho}}{\rho_0}\right) . \qquad (2\text{-}7)$$

The inner product is

$$\langle a | b \rangle = \int_{-\infty}^{\infty} a_1^* b_1 + a_2^* b_2 + a_3^* b_3 + a_4^* b_4 + a_5^* b_5 \, dxdydz . \qquad (2\text{-}8)$$

In the new space our eigenvalue problem, Equation (2-2), becomes

$$M|a\rangle = \omega|a\rangle \tag{2-9}$$

where

$$M = ic \begin{pmatrix} 0 & -\frac{\partial}{\partial z} - \frac{1}{2H} + \frac{1}{\gamma H} & -\frac{\partial}{\partial x} & -\frac{\partial}{\partial y} & 0 \\ -\frac{\partial}{\partial z} + \frac{1}{2H} - \frac{1}{\gamma H} & 0 & 0 & 0 & \frac{\sqrt{\gamma-1}}{H\gamma} \\ -\frac{\partial}{\partial x} & 0 & 0 & 0 & 0 \\ -\frac{\partial}{\partial y} & 0 & 0 & 0 & 0 \\ 0 & -\frac{\sqrt{\gamma-1}}{H\gamma} & 0 & 0 & 0 \end{pmatrix} \tag{2-10}$$

This operator is indeed selfadjoint and we can use all the standard procedures. If, for example, the perturbed configuration at time 0 is $|f\rangle$. At later times the configuration will be†

$$|a\rangle = \int \langle\omega|f\rangle \, |\omega\rangle \, e^{-i\omega t} d\omega \tag{2-11}$$

where the $|\omega\rangle$ are the eigenvectors of M with eigenvalue ω.

† Equation 2-11 symbolically indicates that we must sum over all the eigenstates; due to degeneracy the sum will be a multiple integral.

C. EIGENVECTORS

Direct substitution into (2-10) readily verifies that[7]

$$|k,a\rangle_j = \begin{pmatrix} P_1 & J_0(kr) \\ P_2 & J_0(kr) \\ P_3 & J_1(kr) \\ P_4 & J_0(kr) \end{pmatrix} e^{iaz} \quad , \; j = 1,2,3,4 \qquad (2\text{-}12)$$

is an eigenvector of M if:

$$P_1 = \frac{\omega\left(1 - \left(\frac{\omega_b}{\omega}\right)^2\right)}{ca - i\omega_d} \; , \qquad P_2 = 1$$

$$P_3 = -i\frac{k}{\omega} P_1 \; , \qquad P_4 = -i\frac{\omega_b}{\omega} \qquad (2\text{-}13)$$

$$c^2a^2 = \omega_a^2 - \omega^2 + k^2\left(\left(\frac{\omega_b}{\omega}\right)^2 - 1\right)c^2 \; . \qquad (2\text{-}14)$$

In (2-12) the index j denotes the distinct eigenvectors corresponding to different ω_j solutions of the dispersion relation (2-14) as discussed below. In Equation 13 a can be any real number and k can be any positive real number.

In (2-14) we defined:

$$\omega_a^2 = \gamma^2 g^2/4c^2$$

$$\omega_b^2 = (\gamma-1)g^2/c^2 \qquad (2\text{-}15)$$

$$\omega_d^2 = \omega_a^2 - \omega_b^2$$

By using Equation 2-14 we can convert from the variable pair (k, a) to (ω, a) and we shall do so later.

The eigenvectors are normalized as:

$$ {}_i\langle a,k|k',a'\rangle_j = N^2 \frac{(2\pi)^2}{k} \delta(k-k')\ \delta(a-a')\ \delta_{ij} \qquad (2\text{-}16) $$

with

$$ N^2 = \sum_i |P_i|^2 = \frac{2}{(a^2c^2+\omega_d^2)\omega^2} \left[\omega_b^2(a^2c^2+\omega_d^2) + (\omega_b^2-\omega^2)^2\right] \qquad (2\text{-}17) $$

Since the dispersion (2-14) is a quartic equation for ω, there are four orthogonal eigenvectors, one for each solution of the quartic:

$$ \omega_i = \frac{(-1)^i}{\sqrt{2}} \left[\omega_a^2-(k^2+a^2)c^2 + (-1)^{\left[\frac{i-1}{2}\right]} \left((\omega_a^2-(k^2+a^2)c^2)^2-4k^2\omega_b^2c^2\right)^{1/2}\right]^{1/2} $$

$$ i = 1,2,3,4 \qquad (2\text{-}18) $$

It can be readily shown that for the roots corresponding to the positive sign in the square brackets, $\omega_i^2 \geq \omega_a^2$ i=1,2 and for the negative sign $\omega_i^2 < \omega_b^2$, i = 3, 4.

D. THE INITIAL CONFIGURATION

As the blast wave moves outwardly from a low altitude nuclear explosion it leaves behind most of the energy of the explosion (some of which was initially radiated away) in the very hot fireball and a region surrounding it which is heated to a much smaller degree. By the time the overpressure reaches a value of about .05 the blast wave contains only about 5 percent of the energy of the explosion. The general plan of our calculation is to follow the blast wave until the nonlinear effects are small and we can make use of linearized equations; at such point we shall make use of results obtained earlier which solve the initial value

problem for the linearized equations. It may appear that the point at which the amplitude of the blast wave decays to .05 would be an appropriate time to perform the coupling calculation. Such is not the case however. As the blast wave propagates upwardly through the atmosphere it strengthens and lengthens. A strengthening of the wave is predicted by linear theory but not very accurately; the lengthening of the wave is an inherently nonlinear effect which would not occur at all in linear theory.

A method for calculating the nonlinear propagation of the wave to high altitudes was developed by us and is given in Reference 8. The wave assumes approximately an N-wave shape; that is, it has a shock wave at the leading edge across which the pressure jumps to some large value followed by an approximately linear decrease (with distance behind the shock) to a value below the ambient pressure ending in an abrupt return to ambient. Specifically, we shall take the hydrodynamic variables to be given by

$$|f(0)\rangle = \gamma \frac{A}{c} \frac{1}{R'} \left(1 - \frac{2}{L}(D-R')\right) \begin{pmatrix} 1 \\ \frac{z'}{R'} \\ \frac{r'}{R'} \\ 0 \end{pmatrix} \qquad (2\text{-}19)$$

where A and L are given, as a function of the yield and altitude D of the event, in Reference 8.

We have now, we believe, an accurate description of the wave at some high altitude and it is at this point we shall perform the coupling to the freely propagating gravity waves. At this time the front of the wave is no longer weak but substantial, possibly even considerably larger than one for a large low altitude explosion. The reader may wonder what justification we have for treating the problem in the linear theory from this point on. What we offer is more an excuse than a justification.

While the amplitude of the wave is larger most of the strength is contained in short wavelengths. The content of the wave at wavelengths which, as we shall see later, are primarily responsible for coupling to gravity waves is in fact small. Furthermore, much of the nonlinear lengthening of the pulse has already taken place (the reason for our using the method of Reference 8 to propagate the wave to high altitudes). Thus the content of the wave at the most important wavelengths is small and will change only a little for the rest of the development. We must anticipate, however, some dependence of our results on the altitude at which we choose to do the coupling. Another reason for a coupling altitude dependence of our results is that the method used in Reference 8 calculates only an approximate wave form making no attempt to calculate the details of the change in shape as the wave propagates. We thus believe that Equation (2-19) provides a reasonable initial condition for linearized calculation of the amplitude of the gravity wave response and obtaining the general features of the wave form. Detailed calculations of the wave form would require more accurate nonlinear calculations. It is perhaps surprising that our calculated waveforms agree with the data as well as they do.

Since the eigenvectors $|k,a\rangle_i$ form a complete set, the vector $|f(0)\rangle$ can be expanded as:

$$|f(0)\rangle = \sum_{i=1}^{4} \int dk \int da \, \frac{1}{N^2} \, |k,a\rangle_i \, {}_i\langle k,a|f(0)\rangle \tag{2-20}$$

To obtain the pulse at any later time we write:

$$|f(t)\rangle = \sum_{i=1}^{4} \int dk \int da \, \frac{1}{N^2} \, e^{-i\omega_i t} \, |k,a\rangle_i \, {}_i\langle k,a|f(0)\rangle, \tag{2-21}$$

with ω_i given by Equation 18.

For calculational purposes it is advantageous to use (ω, a) as integration variables. The integral (2-21) can then be written as

$$|f(t)\rangle = \{\int_{-\omega_b}^{\omega_b} d\omega \int_{-\infty}^{+\infty} da + (\int_{-\infty}^{-\omega_a} + \int_{\omega_a}^{\infty})d\omega \int_{\sqrt{\omega^2-\omega_a^2}}^{\sqrt{\omega^2-\omega_a^2}} da\} \frac{Y(\omega,a)}{N^2} |\omega,a\rangle\langle\omega,a|f(0)\rangle \quad (2\text{-}22)$$

where

$$Y(\omega,a) = N^2 \frac{|\omega|}{\omega_b^2-\omega^2} \quad (2\text{-}23)$$

is the Jacobian of the transformation. Note that the sum over different eigenstates is now represented by ω integrals over different ranges, the first term corresponding to i=3,4 and the third and fourth term to i=1 and 2 respectively.

The evaluation of $\langle\omega,a|f(0)\rangle$ has been given in Reference 7. Here we only quote the final result

$$\langle\omega,a|f(0)\rangle = \frac{4\pi A\sqrt{\gamma}}{c\sigma^2} e^{-iaD}[P_1^* (\frac{2}{L\sigma} (\sin\sigma D-\sin\sigma(D-L)) - (\cos\sigma D+\cos\sigma(D-L)))$$

$$+(ia+kP_3^*) \frac{1}{\sigma} (\frac{L-2D}{L} (Si(\sigma D)-Si(\sigma(D-L))) - (\sin\sigma D+\sin\sigma(D-L))$$

$$- \frac{4}{\sigma L} (\cos\sigma D-\cos\sigma(D-L)))] \quad (2\text{-}24)$$

Here

$$\sigma^2 = k^2+a^2 \quad , \quad (2\text{-}25)$$

and Si(x) is the sine integral function. In contrast to the two layer atmosphere considered in Reference 7, σ is always real in the isothermal case.

The overlap function vanishes as $L \to 0$, i.e., in the limit of no source, as it should. It is also fairly easy to show that $\langle \omega, a | f(0) \rangle$ is finite for $\sigma \to 0$ since the quantity in square brackets is proportional to σ^2 in this limit.

From (2-12) and (2-20) we can now evaluate the velocity in the z-direction,

$$\tilde{V}_z = \frac{Re}{\sqrt{\gamma}} \int d\omega \int da \; \langle \omega, a | f(0) \rangle e^{-i(\omega t - az)} \frac{J_0(kr)}{N^2} Y(\omega, a) \tag{2-26}$$

For the radial component of the velocity we obtain

$$\tilde{V}_r = \frac{Re}{\sqrt{\gamma}} \int d\omega \int da \; P_3(\omega, a) \langle \omega, a | f(0) \rangle e^{-i(\omega t - az)} \frac{J_1(kr)}{N^2} Y(\omega, a) \tag{2-27}$$

The corresponding r, z-components of the displacement can be found by numerically integrating $\tilde{V}_z(t)$, $\tilde{V}_r(t)$ or by closed form integration, e.g.

$$\tilde{d}_z = \frac{Re}{\sqrt{\gamma}} \int d\omega \int da \; \frac{i}{\omega} \langle \omega, a | f(0) \rangle e^{-i(\omega t - az)} \frac{J_0(kr)}{N^2} Y(\omega, a) \tag{2-28}$$

The twiddled quantities are related to the observables through a simple exponential factor. To make this relation explicit we write:

$$\hat{V}_i = \frac{\tilde{V}_i}{A\sqrt{\gamma}} \tag{2-29}$$

and we can then show, assuming the scale height is independent of z as was done in obtaining the linearized equations, Equation (2-1):

$$V_i = \frac{\Delta P}{\gamma P} D \exp\left(\frac{z-D}{2H}\right) \hat{V}_i ; \qquad i = z, r \tag{2-30}$$

and $\frac{\Delta P}{P}$ is the relative overpressure at height D. Strictly speaking, Equation 2-30 is incorrect since H depends strongly on z, varying by an order of magnitude. Thus the absolute normalization of the pulse predicted by 2-30 must be modified to incorporate, at least approximately, the varying scale height. To do this, we rewrite 2-30 as:

$$V_i = \frac{\Delta P}{\gamma P} D \exp\left(\frac{z-D}{2H_{eff}}\right) \hat{V}_i; \quad i = z, r. \tag{2-31}$$

In our calculations we determine H_{eff} by the following procedure. We note that the ambient pressure at the height z is

$$P(z) = P_0 e^{-\frac{z}{H(z)}} = P(D)\, e^{-\frac{z-D}{H_{eff}}} \tag{2-32}$$

Thus:

$$1/H_{eff} = \frac{1}{z-D} \ln \frac{P(D)}{P(z)} \tag{2-33}$$

where P(D) and P(z) are taken from tables of atmospheric properties. For example, for z=300 km and D=100km we get H_{eff}=25km. A simpler estimate is to use $H_{eff} = 1/2\ (H(z) + H(D)) = 31.4$ km, resulting in a difference of factor of 2 in the overall normalization.

To evaluate V_i, all that is needed to evaluate $\hat{V}_i$. This can be done either numerically or using any of the available approximation techniques, such as the stationary phase. As we shall see, only the exact calculations are capable of providing the detailed information about the time dependence of the atmospheric motion, while the stationary phase gives some qualitative features of the TID, but does not provide useful quantitative information.

E. EVALUATION OF THE DOUBLE INTEGRAL

The generic form of the integral is (cf. Equation (2-23))

$$V = \int d\omega \int da\; y(\omega,a) e^{-i\omega t} \tag{2-34}$$

$$= \int_{-\omega_b}^{\omega_b} d\omega \int_{-\infty}^{+\infty} da\; y(\omega,a) e^{-i\omega t} + \left(\int_{\omega_a}^{\infty} d\omega + \int_{\infty}^{-\omega_a} d\omega\right) \int_{-\sqrt{\omega^2-\omega_a^2}}^{\sqrt{\omega^2-\omega_a^2}} da\; y(\omega,a) e^{-i\omega t} \tag{2-35}$$

Since the high frequency components of the blast wave do not propagate very far in the atmosphere, it appears reasonable to assume that the second term contributes little at large distances. We can therefore approximate the integral by the first term only. In principle, this evaluation becomes very time consuming if needed for a number of different values of t,z,D,r,L. To improve the speed of the numerical calculations we note that we are interested in V as a function of time. Therefore, we construct tables of the integrals:

$$Y(\omega,T) = \int da\; y(\omega,a) e^{-i\omega t} \tag{2-36}$$

for a fixed t=T we then have

$$V(t) = \int d\omega Y(\omega,T)\; e^{i\omega(T-t)} \quad . \tag{2-37}$$

Once $Y(\omega,T)$ is known to any desired accuracy, the evaluation of V(t) from (2-37) is quite rapid. The results of the numerical calculations are reliable only for small times, i.e., the first few periods after the arrival of the pulse. To calculate for later times it is necessary to develop approximate techniques for the evaluation of the double integral.

The method adopted is that of stationary phase, which has been used by several authors (4). The essential idea of the stationary phase is that the major contribution to an integral of an oscillatory function arises from the point at which the phase is stationary.

To obtain a form amenable to the stationary phase treatment, we note that:

$$Si(x) = f(x)\sin x + g(x)\cos x \tag{2-38}$$

$$J_\upsilon(x) = F(x)\sin x + G(x)\cos x \tag{2-39}$$

where f,g, F,G are functions which we assume have no oscillatory structure. Strickly speaking, this is not correct. For example, in the Bessel function, the argument in the trigonometric functions contains corrections of order 1/x. However, since the stationary phase is an approximation, this probably does not cause large errors.

The phases in the double integral are of the form:

$$\phi = \omega t \pm kR - a(z-D) \pm \alpha d \ , \tag{2-40}$$

where d=D or d=D-L. To obtain the stationary points, we need to calculate the roots a_s, ω_s of the equations.

$$\frac{\partial \phi}{\partial \omega} = 0 \quad , \quad \frac{\partial \phi}{\partial a} = 0 \tag{2-41}$$

This leads to 8th order algebraic equations whose solutions cannot be given in closed form.

Since we know that high frequencies do not propagate easily over large distances, we assume $\omega^2 << \omega_b^2$. With this assumption the dispersion (16) becomes:

$$a^2 = -\left(\frac{\omega_a}{c}\right)^2 + k^2\left(\frac{\omega_b}{\omega}\right)^2 \tag{2-42}$$

and the stationary points are

$$\omega_s \approx \pm \frac{\omega_b t \zeta c}{r\sqrt{c^2t^2-\rho^2}} \approx \frac{\omega_b \zeta}{r}$$

$$a_s \approx \pm \frac{\omega_a}{rc}\sqrt{t^2c^2-\rho^2} \approx \omega_a t/r \qquad (2\text{-}43)$$

$$k_s \approx \frac{\omega_b t \zeta}{r^2}$$

and $\sigma^2 \approx a^2$. Here $\zeta = z-D\pm d$ and $\rho = \omega_a r/\omega_b$

The stationary phase method then consists of approximating the integral

$$I = \int d\omega \int da\ e^{i\phi(\omega,a)} F(\omega,a) \qquad (2\text{-}44)$$

by:

$$I = \sum_s \frac{2\pi}{\left[\frac{\partial^2\phi}{\partial a^2}\Big|_{\omega_s,a_s} \frac{\partial^2\phi(a_s,\omega)}{\partial\omega^2}\Big|_{\omega_s}\right]^{1/2}} F(\omega_s,a_s)\, e^{i(\phi(\omega_s,a_s)+\pi/4)} \qquad (2\text{-}45)$$

and the sum is over all stationary points.

After some tedious algebra:

$$\left[\frac{\partial^2\phi(\omega,a)}{\partial a^2}\Big|_{\omega_s,a_s} \frac{\partial^2\phi(a_s,\omega)}{\partial\omega^2}\Big|_{\omega_s}\right]^{1/2} = \frac{c|a_s|r}{\omega_a\omega_b t}\left(2t^2\omega_a^2 + a_s^2r^2\right)^{1/2} \qquad (2\text{-}46)$$

Let:

$$\zeta_1 = z,\ \zeta_2 = z-2D,\ \zeta_3 = z-L,\ \zeta_4 = z+2D-L \tag{2-47}$$

$$\phi_i^{(+)} = \omega_s(\zeta_i)t - k_s(\zeta_i)R - a_s\zeta_i$$

$$\phi_i^{(-)} = -\omega_s(\zeta_i)t + k_s(\zeta_i)R - a_s\zeta; \tag{2-48}$$

and there are 8 stationary phase points in the integral. The evaluation of the stationary phase integral is fairly rapid, as compared to the exact calculations. However, the stationary phase calculation is possible only at time $t>\rho/c$, and $\rho \geq r$, i.e. after the pulse arrival. For $\gamma = 1.4$, $\rho = 1.108r$ and the stationary phase derivation based on the assumption $\omega^2 << \omega_a^2$ is valid only for $t \gtrsim 1.5\ R/c$ by which time most of the disturbance has died out. Nevertheless, the stationary phase is useful in making qualitative statements about the nature of the oscillatory behavior. For example, the form of the stationary phase ϕ_s suggests that the fastest period of the oscillation is about

$$\omega_s \approx \frac{\omega_b z}{r} \tag{2-49}$$

as is indeed borne out by our exact calculations.

Before proceeding further we discuss other stationary phase treatments found in literature and point out some drawbacks of this method. In the exact calculations the velocity and displacement are related by:

$$V = \mathrm{Re}\left(\int d\omega\ F(\omega)e^{i\omega t}\right) \tag{2-50}$$

$$d = \mathrm{Re}\left(\int d\omega\ \frac{F(\omega)}{i\omega}\ e^{i\omega t}\right) \tag{2-51}$$

and it is a standard assumption in the literature that if both V, d are calculated from the stationary phase approximation to these integrals then the relation

$$d = \int dt V(t) \tag{2-52}$$

is satisfied. We show (in Appendix A) that this is not exactly correct and it is necessary to decide which integral is (better) approximated by the stationary phase. The difference in evaluating d from (2-51) or from (2-52) depends on the structure of the dispersion relation and the form of the function $F(\omega)$ and the accuracy of the stationary phase approximation.

A related problem is the fact that the stationary phase approximation does not vanish as $L \to 0$, i.e., in the limit of no source. Both these difficulties can be remedied by including higher order terms in the stationary phase expansion, thus satisfying the relation to any arbitrary accuracy. However, the evaluation of the higher order terms involves some extremely complicated algebraic manipulations (for the dispersion relation (2-16) considered here) and is somewhat labor prohibitive.

A standard stationary phase treatment in the literature is carried out on the Green's function.[5] We feel that such a treatment is inconsistent for two reasons. First, the stationary phase Green's function is used in an integral over time which yields the resultant displacement and velocities. As indicated in Appendix A, this may lead to significant, and more importantly uncontrolled errors, thus diminishing the usefulness of such calculations. Second, in the Green's function evaluation, the stationary points are independent of the source, contrary to our results. A more detailed investigation is needed to determine the accuracy of these approximate treatments.

F. NUMERICAL CALCULATIONS

To investigate the possible approaches to calculating the atmospheric gravity waves we have developed two computer codes. The first one evaluates V_z, V_r, d_z, d_r as functions of time for fixed r, D, L exactly from Equations (2-26) and (2-27) and includes also the high frequency ($\omega^2 > \omega_a^2$) contributions. The second code calculates V_z, d_z, V_r, d_r using the stationary phase methods. The calculations were carried out for a range of radial distance r = (1000 - 4000) km and yields Y ranging from 1 kT to 30 MT at observation height z = 300 km. In most calculations the pulse was coupled at D = 100 km and the value of γ = 1.4 was used. Our calculations are normalized as in Equation (2-31) and c = 334 m/sec.

In order to test our codes we have carried out calculations in the region where the pulse originates. Although the calculation is quite time consuming numerically and requires the inclusion of the high frequency parts of the integral, we have been able to reproduce successfully the initial pulse. We have also tested the importance of including the high-frequency contribution to the mode sum. For large radii (r > 1000 km), this contribution turns out to be negligible for all times $t \geq R/c$, $R^2 = r^2+z^2$.

The next calculation we wish to discuss is the comparison of the stationary phase and the exact numerical calculations illustrated in Figure 1. As is readily evident from these results, the stationary phase is quite reliable in predicting the general time dependence of the gravity waves even at fairly early times. However, the stationary phase is totally unreliable in predicting the amplitude of the gravity wave response, except at very late times (after 3 or 4 periods). This is unsatisfactory since by this time the disturbance has essentially died out. At early times, the amplitudes predicted by the stationary phase are

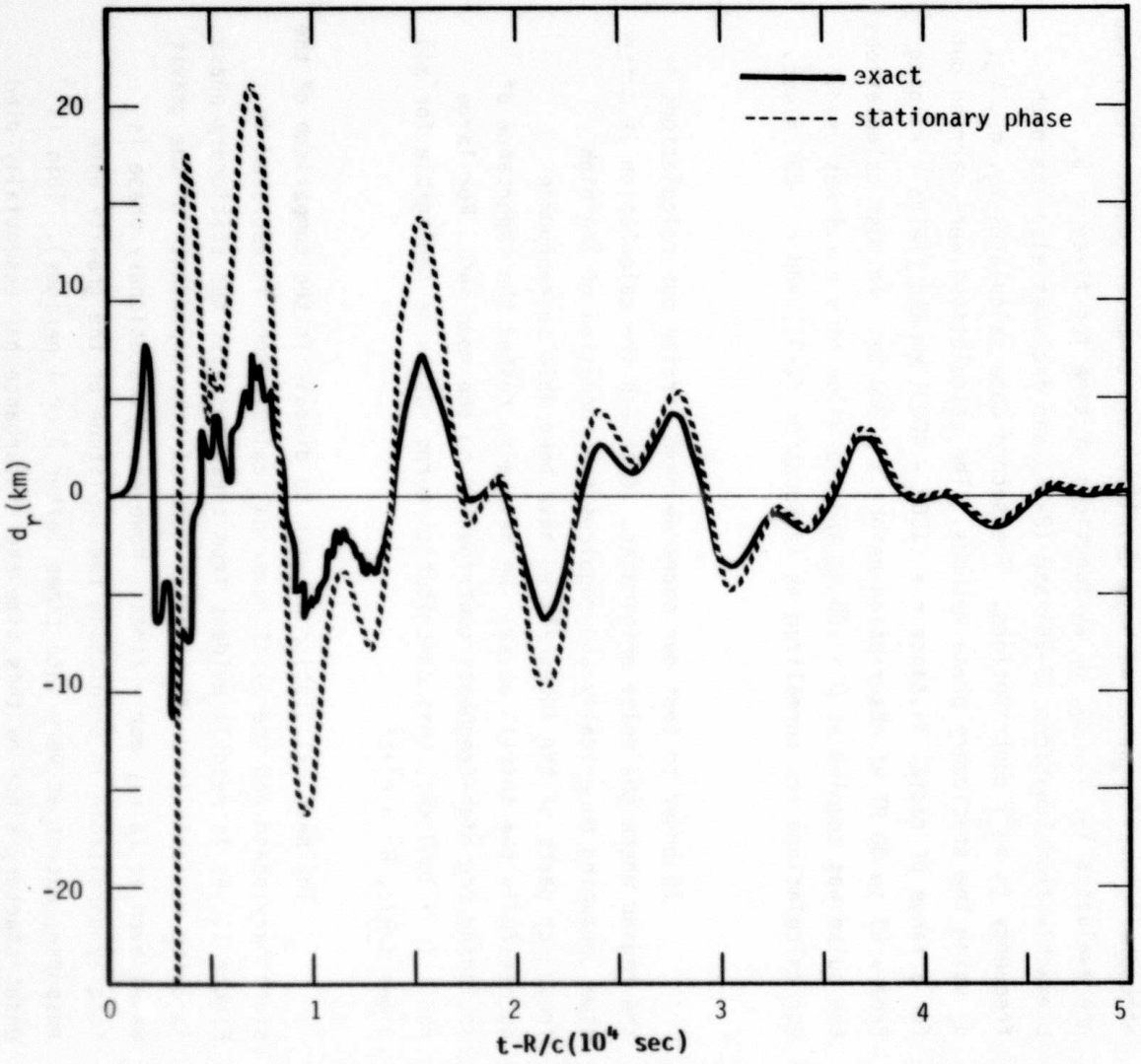

Figure 1. Radial displacement $d_r(t)$ plotted vs. time t. Comparison of exact and stationary phase calculations at z = 300 km, r = 4000 km, and Y = 1 MT.

several orders of magnitude greater than the exact calculations and no stationary phase calculations can be carried out for $t < \omega_a r/\omega_b c$. This suggests that in order to understand the early time behavior of gravity waves it is necessary to carry out exact calculations and the stationary phase is qualitative at best.

With this in mind, we set out to investigate numerically the properties of the gravity wave response as functions of the yield, horizontal distance and γ and compared with observations. In the first set of calculations we calculated the displacement d_r for r=1000, 2000, and 4000 km (i.e. r=R) for the yield Y = 10MT. The results show an initial outward displacement of the atmosphere of about 20-30 km, its magnitude essentially independent of the horizontal distance, followed by an inward displacement whose amplitude decreases with R as 1/R. The period of oscillations increases linearly with R, in agreement with the stationary phase analysis and observations. These results are illustrated in Figure 2 where we plot $d_r(\tau)$, $t = \tau R/c$. Note that the response is essentially zero for $\tau<1$, i.e., prior to the pulse arrival, as it should be. An important information relevant to test detection is the dependence of the gravity wave response on the yield of the weapon exploded. This dependence does not follow trivially from the formal expressions since different yields correspond to different A and L, neither of which have a simple yield dependence. We have carried out exact numerical calculations for yields from 1kT to 30 MT. Some of these calculations are plotted in Figures 3 and 4 where we plot $d_r(t)/Y$ for r = 1000 and 4000 km and Y = .1MT - 30 MT. It is readily seen that in the first period $d_r(t)$ is very nearly proportional to the yield. The yield scaled curves begin to differ at later times. The linear dependence on yield remains valid at later times for the maximum amplitudes, however. The absolute displacements $d_r(t)$ are plotted in Figure 5, for Y=1kT and 10 kT at r=2000 km. The calculated yield dependence of the response cannot be readily deduced from

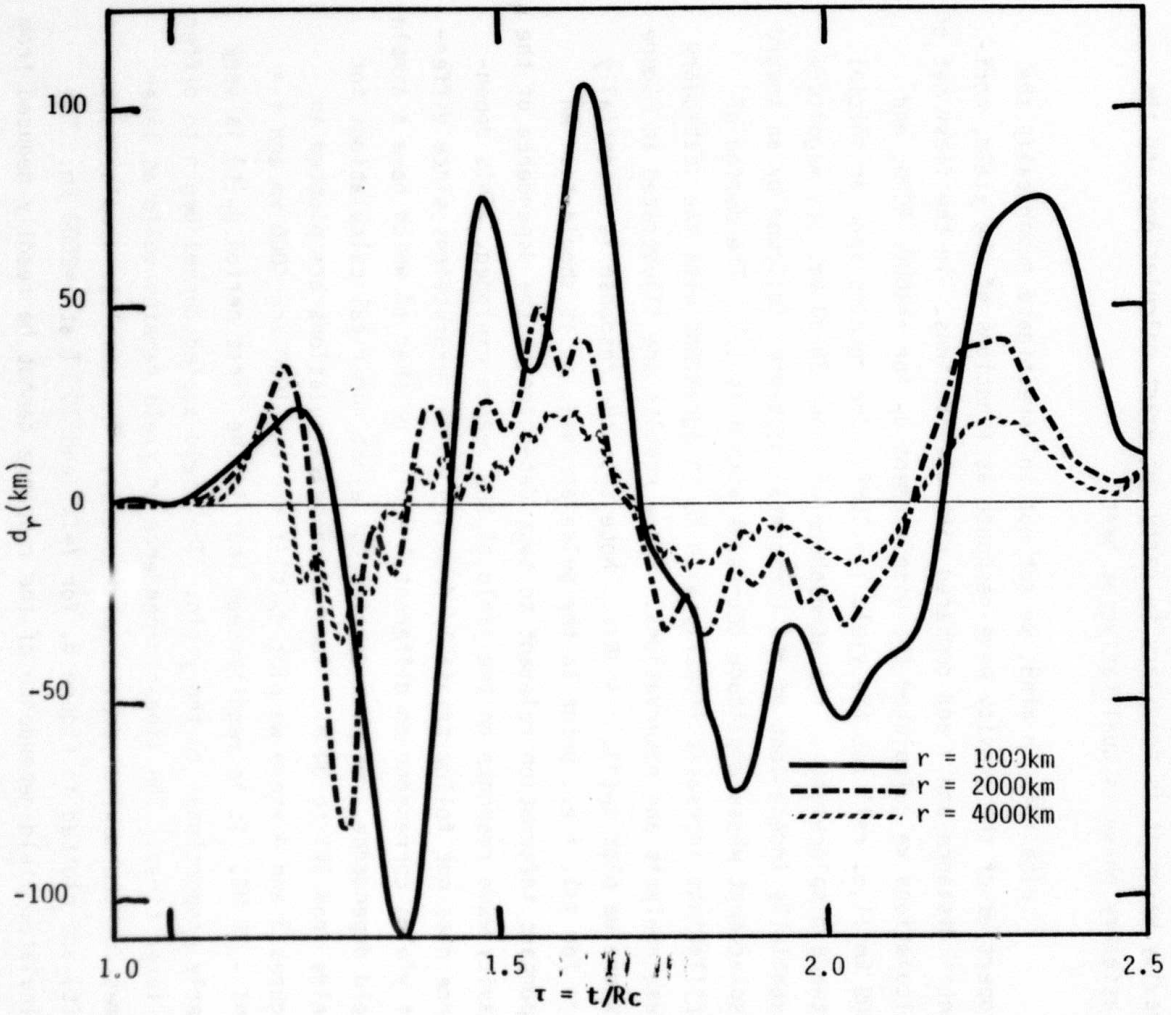

Figure 2. Radial displacements d_r for several values of r, z = 300 km and Y = 10 MT.

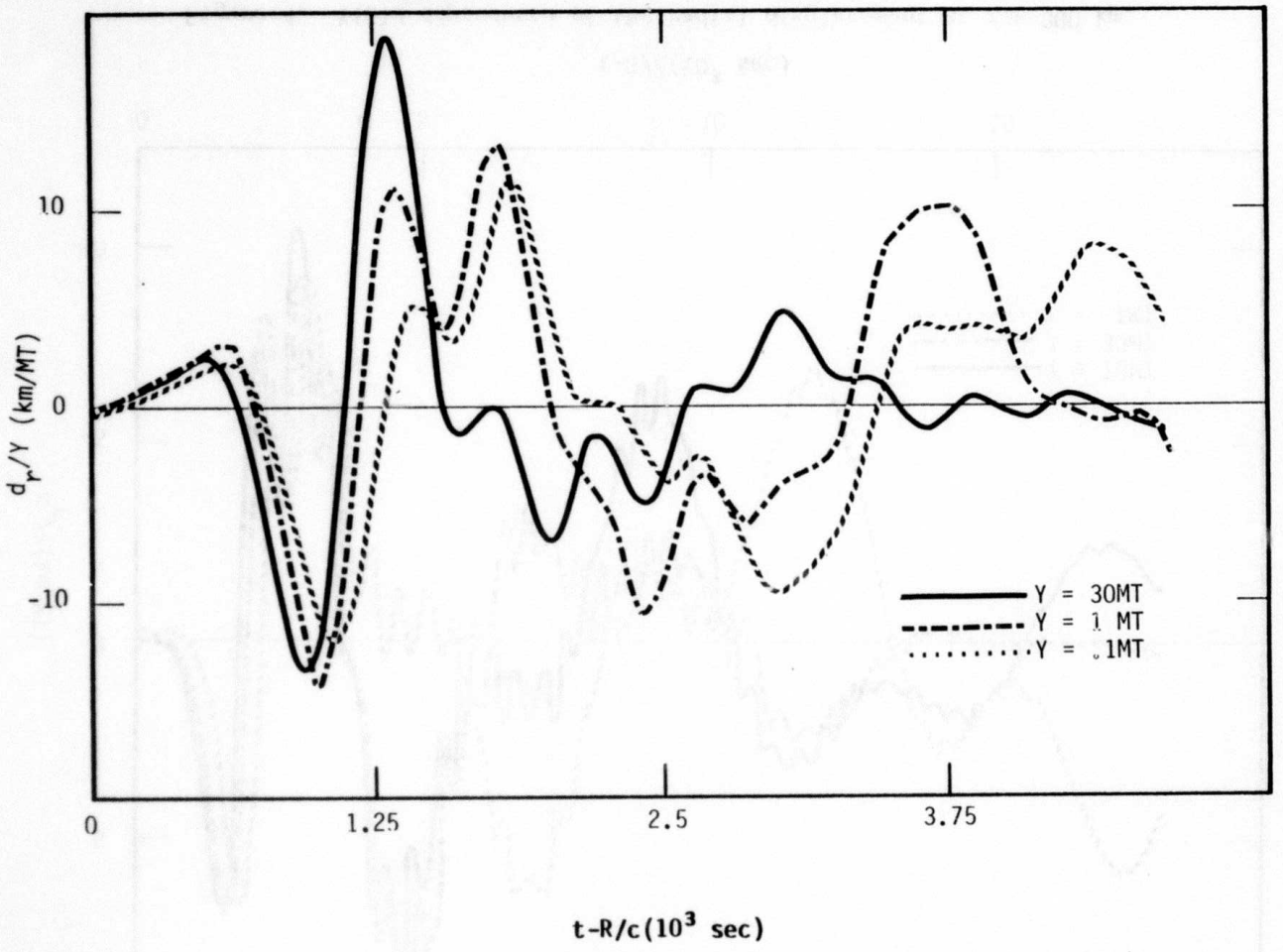

Figure 3. Yield dependence of the radial displacement at z = 300 km, r = 1000 km.

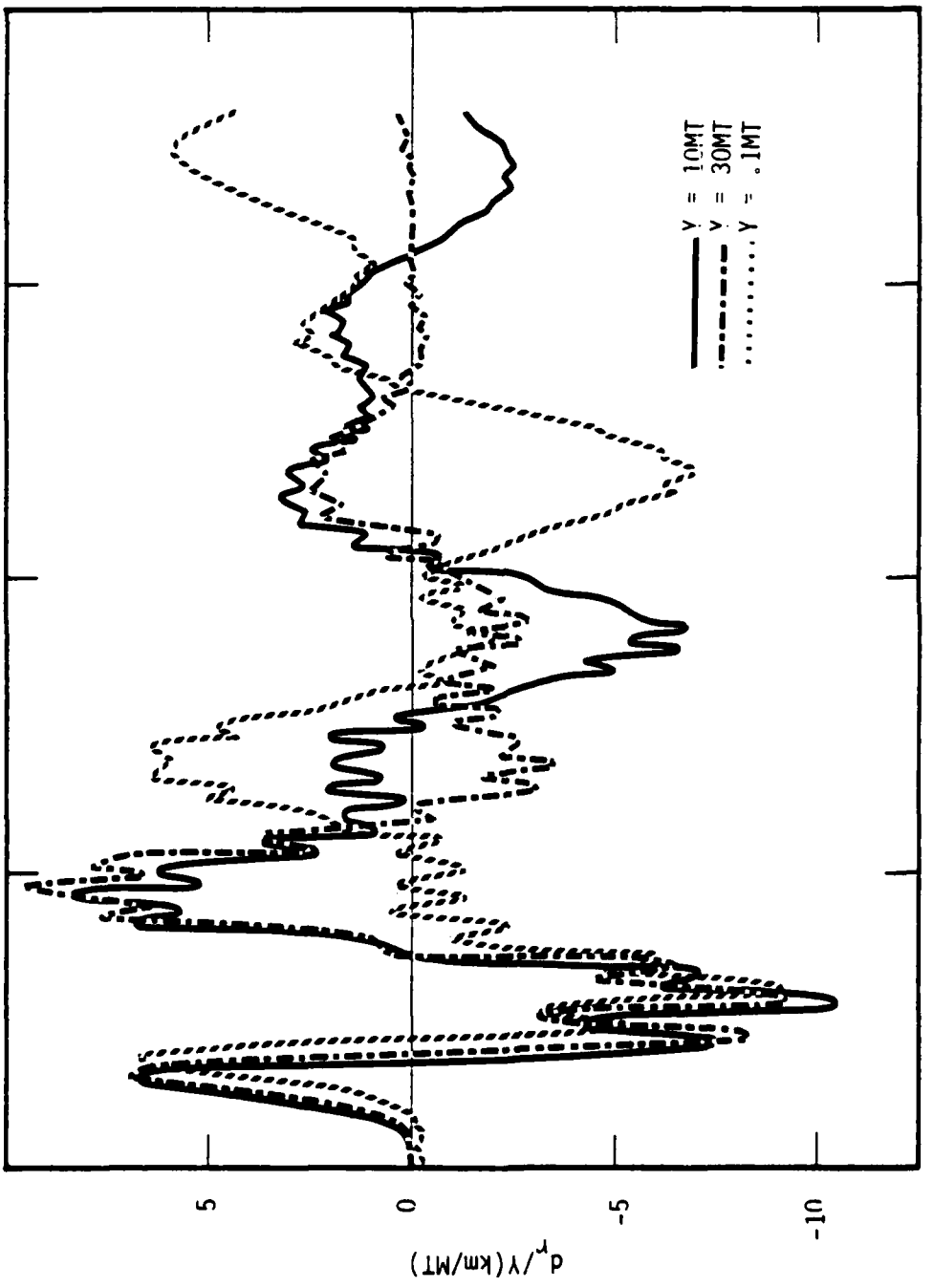

Figure 4. Yield dependence of the radial displacement at z = 300 km, r = 4000 km.

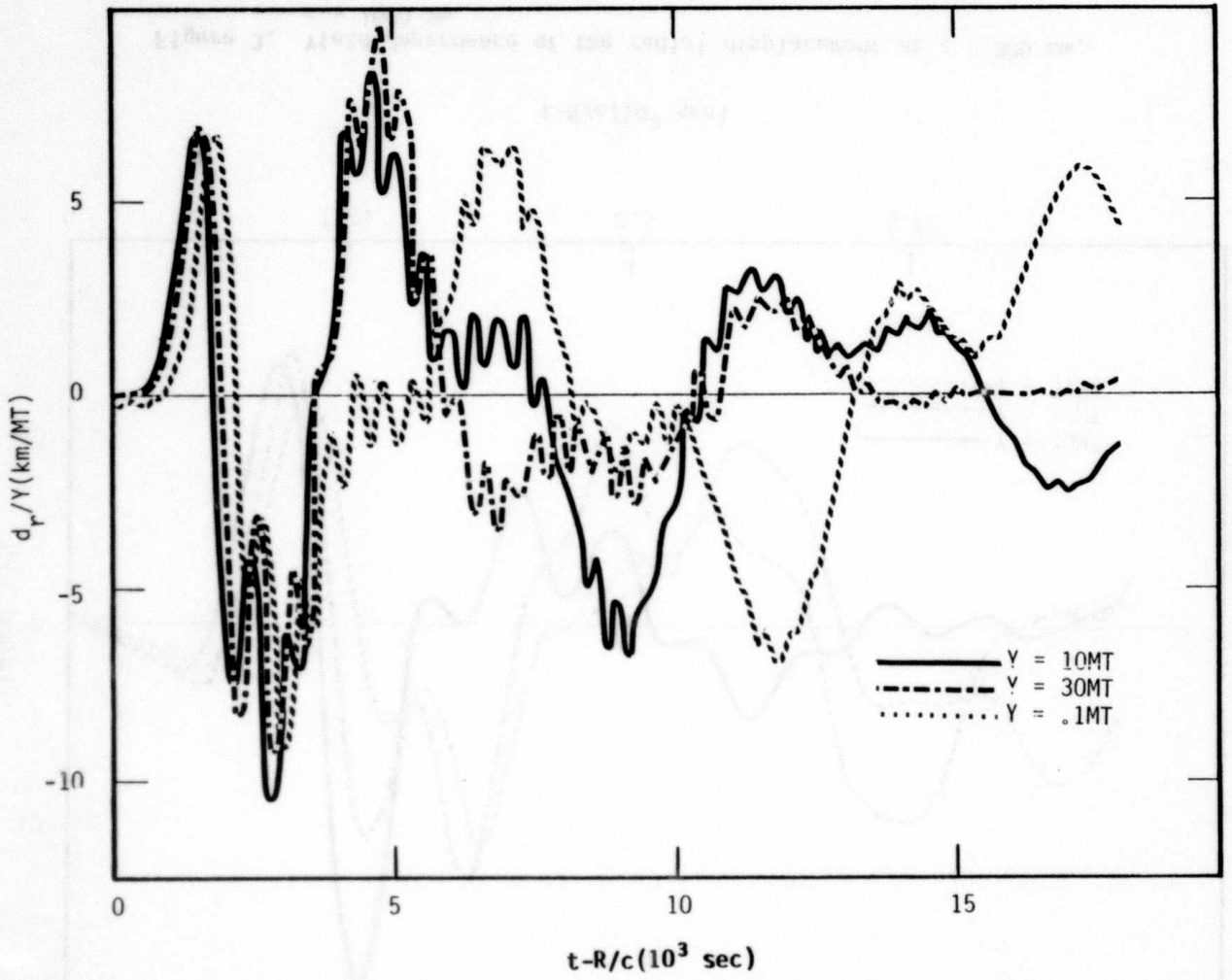

Figure 4. Yield dependence of the radial displacement at z = 300 km, r = 4000 km.

either the exact equations or the stationary phase calculations. Another numerical analysis has been carried out to study the γ dependence. Our results indicate that the period of the gravity wave response is approximately proportional to $1/\sqrt{\gamma}-1$ in agreement with the stationary phase prediction, and the amplitude is roughly independent of γ. This is illustrated in Figure 6 for $\gamma = 1.67$ and $\gamma = 2$.

For the calculated radial distances, the vertical displacement $d_z(t)$ is found negligible compared to d_r. For observation carried out at and magnetic dip angle and ϕ, the angle of propagation relative to the magnetic meridian, the vertical height variation is then

$$h(t) \sim d_r(t)\ \sin 2\theta \cos\phi/2.$$

This gives variations in height calculated at Tonga (θ=-41.5°, ϕ=8.1°, r= 3900 km) for the megaton range Housatonic test of order 20-40 km, in agreement with reported observations.[1-5] It should be noted that for bursts in the 1 kT range, the calculated height variations are several meters, well below the sensitivity of the standard ionosond observations and probably well masked by the noise due to ionosphere motion caused by other (natural) mechanisms. Thus it is not likely that the gravity wave can be used as a reliable guide in determining the yield of the weapon exploded for low yield (Y<10kT).

In all the calculations above we had coupled the initial pulse at D=100 km. This is an arbitrarily chosen altitude which may be motivated by the fact that the atmosphere is almost discontinuous at this height. The calculation of $|f(0)>$ using methods of Reference 7 should be reasonable below this height since we expect the pulse to contain very little of low frequency components. We also carried out calculations for D = 150 and 200 km. The calculations indicate a strong dependence on D which is evidently associated with the almost discontinuous behavior of the atmosphere around D = 100 km, which changes rapidly the values of A

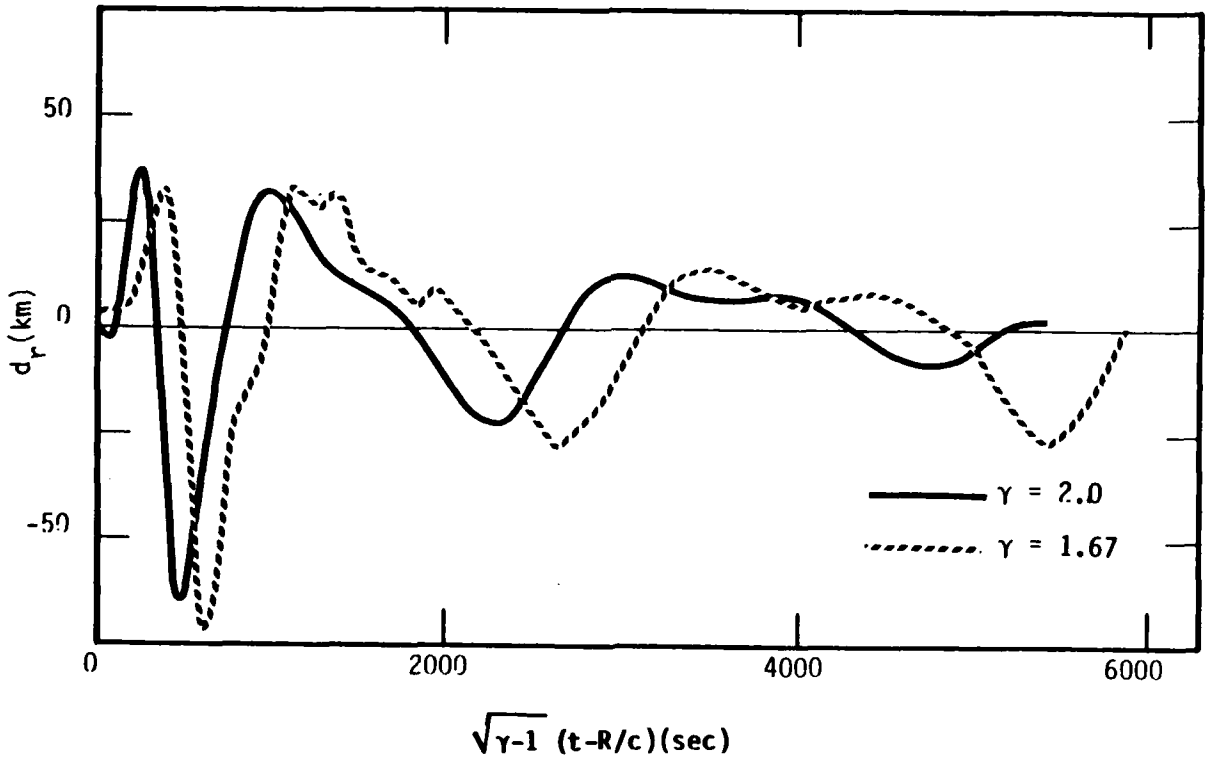

Figure 6. γ dependence of the radial displacement at z = 300 km, r = 2000 km and Y = 10 MT.

and L calculated in the nonlinear model of Reference 8 which are used as input in present calculations. It should be noted that $|f(0)\rangle$ is not a solution of the linearized equations of motion so that the strong D-dependence is not entirely unexpected. In all calculations of the D-dependence, the best agreement is in the size and position of the first peak and the choice of D=100km for our other calculations is more motivated by the agreement with observations then rigorous arguments. Whether this problem can be corrected by using a two layer atmospheric model as outlined in Appendix B or some other means requires further numerical work.

SECTION 3
RISING FIREBALL AS A SOURCE OF GRAVITY WAVES

A. INTRODUCTION

Calculations in the previous section indicate that observed gravity waves from large yield, low altitude nuclear explosions can be produced by the source which provides a high altitude blast wave, namely the initial rapid release of energy at the burst location. While it has long been recognized that nuclear explosions produce distant gravity waves, the details of the source mechanism and its relation to amplitude and time history of the observed gravity wave have not before been firmly connected.

While it has been accepted that the energy source is important, it has been suggested by several authors that the fireball, which is subsequently produced by the energy release, undergoes motion which may also be a significant source for gravity waves.[9,10,11] The fireball is formed within seconds of the burst and it consists of a nearly spherical hot region of greatly reduced density which is approximately in pressure equilibrium with the surrounding cool air. However due to the ambient density stratification there is a net buoyant force on the fireball which causes an initial upward acceleration and a subsequent rise at roughly a constant velocity. The complex details of the fireball rise dynamics include entrainment of cooler air, vortex formation and expansion due to the decrease in ambient pressure with increasing altitudes. The fireball motion does not cease immediately upon reaching its equilibrium altitude,

rather it tends to overshoot this altitude and oscillate about it at approximately the Brunt period. At the same time that the fireball oscillates around the equilibrium altitude, it also expands and contracts in unison due to stratification of the ambient pressure.

In this section we will model several aspects of the fireball motion in order to find the significance of such motion as sources for gravity waves relative to the blast wave source. This will be done using two different models for fireball rise at a constant velocity along with models for fireball oscillation about the equilibrium altitude and for fireball radial expansion and contraction near the equilibrium altitude.

It will be concluded that for the liner theory used, while the fireball motion does indeed act as a gravity wave source, this source mechanism is not important when compared to the initial deposition of energy which produces the blast wave so that fireball motion can be ignored for the purposes of gravity wave production.

B. BACKGROUND

A low altitude nuclear burst quickly dumps energy into a localized region which is approximately spherical. A portion of this energy is radiated away in the form of waves, linear and nonlinear, in both the acoustic and gravity wave frequencies. In the previous section the gravity wave from the blast wave produced by the initial energy deposition was calculated. However after the blast wave has departed from the immediate region of the burst there remains a fireball which undergoes motion which can serve as an additional source for gravity waves. The fireball is formed within seconds of a nuclear explosion and it consists of a heated region of a debris-air mixture which is approximately in pressure equilibrium with the surrounding cooler air. The fireball temperature is about 1 eV and the density is about 10% of ambient. The fireball volume is proportional to the yield so the radius "a" scales like

$$a = 10^5 \, (Y_{MT})^{1/3} \quad \text{(cm)} \tag{3-1}$$

so a 1 MT burst gives a radius of about 1 km.

Since the underdense fireball resides in the stratified atmosphere, there is a buoyant force which tends to cause the heated region to rise. The dynamics of fireball rise include the interaction of the buoyant force with the distortion of the fireball which entrains cooler air and forms a vortex ring. The net effect of this complex behaviour is a gross rise of the original fireball material at a velocity which is nearly constant and is approximately

$$V = \sqrt{ag\beta} \tag{3-2}$$

where g is the acceleration of gravity and β is a measure of density defect of the fireball $\beta = (\rho_0 - \rho)/\rho_0$. This velocity is that appropriate to thermal rise which was given by Scorer.[12]

The flow outside a couple of fireball radii is approximately that seen around an object rising at constant velocity. At smaller radii the features we see are much more complex. However, since the size of this region is small compared to the wavelengths of distant gravity waves, we expect that the details of the motion will not be important in dictating the general character of that gravity wave.

Fireball rise from a 1 MT burst continues for a few hundred seconds until it reaches such an altitude that the density of the expanding fireball equals that of the ambient air. This stabilization altitude (~ 20 km for a 1 MT burst) is dictated by the yield. The fireball does not immediately settle at the stabilization altitude but tends to oscillate about it after an initial overshoot of the order of a scale height.

This oscillation takes place at about the Brunt frequency and may continue for a few cycles. At the same time the fireball is bobbing up and down, it also undergoes radial expansion and contraction. The motion of the fireball about the stabilization altitude will act as a source for gravity wave generation.

To date there has not been a convincing calculation of the extent to which fireball rise is a source of gravity wave. Pierce[10] has presented a formalism which allows gravity wave source terms to be included in the equations in terms of moments of an excluded region such as the fireball. However no examples have been worked out. Murphy and Kahalas[11] have discussed some features of fireball rise sources but again no calculations have been made. The work of Tolstoy and Lau[13], although restricted, is the only example of an attempt to find the quantitative relation between fireball rise and gravity waves.

Tolstoy and Lau have solved for the distant effects of a force source moving upward at constant velocity in an incompressible medium which is bounded by rigid horizontal surfaces at z=0 and z=500 km. The solution is expressed as the sum over the infinite set of modes where the coefficients are evaluated in terms of source characteristics. They find that for a 1 MT surface burst at a range of 10,000 km and an altitude of 250 km vertical displacements of about 5 meters will be generated. The amplitude is found to scale like $(\text{yield})^{5/3}$. An amplitude of 5 meters is quite small compared to observed displacements of tens of kilometers for large yield bursts. Furthermore the time behavior of Tolstoy and Lau's displacement indicates that a period of about 20 minutes dominates the behavior. This behavior is difficult to understand since the Brunt period is ~ 4 min so the dominant period would be expected to be Brunt Period × (R/z) ~ 160 minutes. The authors further calculate the gravity wave effects from a mass injection source (referred to as an explosive source) which gives a gravity wave amplitude which scales like

(yield)$^{1/3}$. It is found that for low-altitude bursts the fireball rise mechanism dominates for yields greater than 1 MT. However the authors point out that an energy injection source will produce a gravity wave amplitude which scales like the yield but no comparison is made with the fireball rise mechanism.

The force source used by Tolstoy and Lau was drawn from work by Warren[14] who calculated the force on objects moving at constant velocity in a stratified incompressible inviscid medium. The force on the objects results exclusively from the stratification of the medium. Warren found that a sphere of radius "a" moving at a velocity V in a medium of density ρ_0 and scale height H requires a sustaining force of

$$F = \frac{\rho_0 \, a^4 \, g}{H} R_d(\nu) \qquad (3\text{-}3)$$

where R_d is a function of velocity, through

$$\nu = \frac{a}{\pi V} \sqrt{\frac{g}{H}} \quad . \qquad (3\text{-}4)$$

For a sphere, R_d is a function which peaks at about 1 for $\nu \approx 0.8$ and is proportional to ν^2 for small ν. This force is referred to as the wave resistance because the energy expended through it is radiated away as gravity waves. It should be noted that F peaks ($\nu = 0.8$) when the time for the fireball to rise a diameter (2a/V) is approximately equal to the Brunt period ($\sqrt{g/H}/2\pi$ for incompressible fluids). Since the buoyant force is at most

$$B_{max} = 4\pi \, \rho_0 \, a^3/3 \, , \qquad (3\text{-}5)$$

the wave resistance is generally less than the buoyant since B/F = 4H/a and H is about 5 km at low altitudes.

Elements of Warren's theory have been verified by experiments by Mowbray and Rarity.[15] In these experiments, a sphere in a stratified medium was moved at a constant velocity while looking for evidence of gravity waves. It was found that no observable wave pattern was set up if the velocity was too great (in Warren's terms $\nu < 0.2$ gave no pattern) but that a smaller velocity (corresponding to $\nu \approx 0.8$) gives rise to a good wave pattern with periods suitably related to the Brunt period.

Other experiments by McLaren, Pierce, Fohl and Murphy[16] are relevant to the generation of gravity waves. These experiments consisted of the release of underdense fluid elements in a stratified medium with subsequent observations of fluid motion well away from the source. The results indicate no gravity waves are generated during the rise phase of the motion. However gravity waves are generated following the rise when the sample fluid element oscillates approximately two times about its stabilization height. It is not clear that the failure to generate waves during the rise is in contradiction to Warren's theory since inadequate information is provided to find a value of ν for comparison. Furthermore it is not obvious that a solid body under an external force should generate the same waves as a miscible fluid element moving at the same velocity under strictly hydrodynamic forces. In any case, the results of McLaren et al., indicate that the oscillations about the stabilization altitude should be considered as a gravity wave source as an element of the fireball rise mechanism.

C. GRAVITY WAVE THEORY

The hydrodynamic equations of motion of a perfect gas in the presence of sources can be written as

$$\frac{\partial \rho}{\partial t} + \vec{V} \cdot \nabla \rho + \rho \nabla \cdot \vec{V} = \rho Q$$

$$\rho \frac{\partial \vec{V}}{\partial t} + \rho(\vec{V} \cdot \vec{\nabla}) \vec{V} - \rho \vec{g} + \nabla p = \rho \vec{F} \tag{3-6}$$

$$\frac{\partial}{\partial t} (p\rho^{-\gamma}) + \vec{V} \cdot \nabla (p\rho^{-\gamma}) = (\gamma - 1) \rho^{1-\gamma} S$$

Where Q is a mass source (sec^{-1}), $\vec{F}$ is an acceleration source (cm/sec^2) and S is a heat source (ergs/gm/sec). When these equations are linearized in an exponential atmosphere of scale height H with constant sound speed c, the Fourier transform of the relative pressure perturbation can be written as

$$\nabla^2 \left(\frac{\hat{\delta p}}{p}\right) + \frac{\omega_b^2}{\omega^2 - \omega_b^2} \frac{\partial^2}{\partial z^2} \left(\frac{\hat{\delta p}}{p}\right) - \frac{\omega^2}{H(\omega^2 - \omega_b^2)} \frac{\partial}{\partial z} \left(\frac{\hat{\delta p}}{p}\right) + \frac{\omega^4}{4(\omega^2 - \omega_b^2) H^2 \omega_a^2} \left(\frac{\hat{\delta p}}{p}\right)$$

$$= \frac{1}{gH} \left\{ \nabla \cdot \hat{\vec{F}} + \frac{\omega_b^2}{\omega^2 - \omega_b^2} \frac{\partial \hat{F}_z}{\partial z} - \frac{\omega^2 \omega_b^2}{g^2(\gamma - 1)(\omega^2 - \omega_b^2)} \hat{F}_z \right\} \tag{3-7}$$

$$+ \frac{i\omega}{g^2 H^2} \left\{ \left(1 - \frac{\omega^2}{(\omega^2 - \omega_b^2)\gamma}\right) \hat{S} + \frac{H\omega_b^2}{\omega^2 - \omega_b^2} \frac{\partial \hat{S}}{\partial z} \right\} + \frac{i\omega}{gH} \hat{Q}$$

$$\equiv \hat{M}$$

where ω_b is the Brunt frequency and ω_a is the acoustic cutoff frequency defined by Equation (2-15).

The formal solution for the pressure pulse resulting from a source M can be written as

$$\frac{\delta p}{p} = e^{z/2H} \int d\vec{r}' \; e^{-z'/2H} \int d\tau \; G(|\vec{r}-\vec{r}'|, \tau) \; M(\vec{r}', t-\tau) \qquad (3\text{-}8)$$

where G is the Green's function for the pressure equation. In general there is no closed form solution for the time domain Green's function However the behavior in the limit of low frequencies, $\omega \ll \omega_b$, is readily expressed as

$$G_{LF} = - \frac{\omega_b}{4\pi R} J_0 \left(\omega_c \; (t^2-(R/c)^2)^{1/2}\right) \; \theta(t-R/c) \qquad (3\text{-}9)$$

where the characteristic late time frequency is

$$\omega_c = \frac{z-z'}{R} \cdot \omega_b$$

for a source to observation range of R and sound speed c. The function θ is a unit step function which allows no response until $t \geq R/c$. While the low frequency Green's function will not accurately reproduce behavior for times near R/c, at observation locations for which $z \ll r$ the later time behavior is well represented. This has been verified in a previous report.[6] As a result, since we are interested in behavior at points at thousands of kilometer ground range from the source, but at ionospheric heights, we feel that the low frequency limit is a useful tool for exploring the implications of different source models.

The source function M, in the low frequency regime can be expressed in the time domain as a rather simple function of Q, $\vec{F}$ and S when it is noted that $i\omega \rightarrow - \frac{\partial}{\partial t}$. Thus for $\omega \ll \omega_b$ we find

$$M_{LF} \rightarrow \frac{1}{gH}\left\{\frac{\partial F_x}{\partial x}+\frac{\partial F_y}{\partial y}+\frac{1}{\omega_b^2}\frac{\partial^3 F_z}{\partial z\,\partial t^2}-\frac{1}{g(\gamma-1)}\frac{\partial^2 F_z}{\partial t^2}\right\}$$

$$-\frac{1}{g^2H^2}\left\{\frac{\partial S}{\partial t}-H\frac{\partial^2 S}{\partial t\,\partial z}\right\}-\frac{1}{gH}\left\{\frac{\partial Q}{\partial t}\right\} \tag{3-11}$$

A useful example of a low frequency response is provided by a source which provides, in the acoustic range, an N-wave pressure fluctuation. As shown in that previous report[17] such a source of temporal length T_0 gives a pulse of the form

$$\frac{\delta p}{p} = A\,\frac{e^{z/2H}}{4\pi R}\left\{N(t-R/c)\right.$$

$$\left.-\frac{\omega_b\,(t-T_0/2)\omega_c T_0^{\,2}}{6\left((t-T_0/2)^2-(R/c)^2\right)^{1/2}}\,J_1\left[\omega_c(t-T_0/2)^2-(R/c)^2\right)^{1/2}\right\} \tag{3-12}$$

where N(t) is a unit amplitude N-wave and the normalization A can be fixed in terms of the N-wave amplitude at any location. Thus if the N-wave has an amplitude $(\delta p/p)_0$ at a vertical location z_0, the low frequency gravity wave associated with the same source will have a peak value of

$$\left(\frac{\delta p}{p}\right)_{max} \approx \left(\frac{\delta p}{p}\right)_0 \frac{z_0}{R}\,e^{\frac{z-z_0}{2H}}\cdot\frac{\omega_b\,\omega_c^2\,T_0^2}{12}\,\frac{R}{c} \tag{3-13}$$

for a time t just after R/c. Note that $\left(\frac{\delta p}{p}\right)_0$ in this equation is the same as $\frac{\Delta P}{P}$ in Equation (2-30). This example will serve as a useful standard against which to compare the effects of other sources.

D. RISING FIREBALL MODELS

In this subsection we will present, in the context of gravity wave theory, solutions for a set of source models which simulate several aspects of fireball motion. These gravity waves will be compared with those from a blast wave source in order to establish the dominant source mechanism for gravity waves from nuclear explosions. The models include two which provide fireball rise, one which simulates the vertical bobbing motion about the stabilization altitude and one which describes the coherent radial oscillations, or breathing, while the fireball oscillates around the stabilization altitude.

D.1. Moving Source of Force

Initially we will consider the source model used by Tolstoy and Lau. This is a point source of force in the vertical direction which moves at a constant velocity V for an interval of time T. The acceleration per unit volume imposed is

$$F_z = \frac{\mathcal{F}}{\rho} \cdot \delta(x)\ \delta(y)\ \delta(z-Vt)\ [\theta(t) - \theta(t-T)] \qquad (3\text{-}14)$$

where θ is the unit step function. Here $\mathcal{F}$ will be taken as the net force on a sphere moving at uniform velocity through a stratified medium as given by Warren. The source can be considered as a point because the gravity wave wavelengths of interest greatly exceed the fireball size.

The low frequency source M_{LF} contains a term for a force source which is proportional to the second time derivative as well as the z-derivative of this expression. Since the source region is small and the force has a single sign, we can neglect the z-derivative contribution. Therefore the low-frequency pressure fluctuations from this source mechanism is

$$\frac{\delta p}{p} = e^{z/2H} \int dz' \, e^{-z'/2H} \int_{R/c}^{\infty} d\tau \left[- \frac{\omega_b}{4\pi R} J_0 \left(\omega_c \sqrt{\tau^2 - R^2/c^2} \right) \right]$$

$$\cdot \left(- \frac{1}{g^2 H (\gamma - 1)} \right) \left(\frac{\mathcal{F}}{\rho} \right) \Big\{ \delta(z' - (t-\tau)V) \left[\delta'(t-\tau) - \delta'(t-T-\tau) \right] \qquad 3\text{-}15)$$

$$- 2V\delta'(z-(t-\tau)V) \left[\delta(t-\tau) - \delta(t-T-\tau) \right]$$

$$+ \frac{\delta''(t-\tau-z/V)}{|V|} \left[\theta(t-\tau) - \theta(t-T-\tau) \right] \Big\}$$

The three terms lead to contributions which are of the form

$$\frac{\delta p}{p} = \frac{e^{z/2H} \, \omega_b \, \mathcal{F}}{4\pi(\gamma-1) \, g^2 H \rho} \cdot$$

$$\left\{ - \frac{e^{-z'/2H} \, J_1 \left(\omega_c \sqrt{t^2 - R^2/c^2} \right) \omega_c \, t'}{r\sqrt{t^2 - R^2/c^2}} \, \theta(t' - R/c) \right\} \Bigg|_{\substack{z'=0 \\ t'=0}}^{\substack{z'=VT \\ t'=t-T}}$$

$$- \frac{2V \, e^{z/2H} \, \omega_b \mathcal{F}}{4\pi(\gamma-1) \, g^2 H \rho} \cdot$$

$$\left\{ - \frac{\partial}{\partial z'} \left(\frac{e^{-z'/2H}}{R} J_0 \left(\omega_c \sqrt{t'^2 - R^2/c^2} \right) \right) \theta(t' - R/c) \right\} \Bigg|_{\substack{z'=0 \\ t'=t}}^{\substack{z'=VT \\ t'=t-T}}$$

$$+ \frac{e^{z/2H} \, \omega_b \mathcal{F}}{4\pi(\gamma-1) g^2 H \rho |V|} \int_0^{\mathrm{Min}(VT, V(t-R/c))} dz' \, \frac{e^{-z'/2H}}{R}$$

$$\left[\frac{\partial^2}{\partial \tau^2} \left(J_0 \left(\omega_c \sqrt{\tau - R^2/c^2} \right) \right) \right] \Big|_{\tau = t - z'/V} \qquad (3\text{-}16)$$

where $R \equiv [r^2 + (z-z')^2]^{1/2}$. Note that the third term begins at zero at $t = R/c$ and grows linearly in time at early time while the other two terms have their peak (although this is not completely obvious) at t immediately following R/c. The first two terms are obtained by evaluation of the difference of the expressions at the indicated values of z' and t'. If $t < R/c + T$, then only the upper values are used since the second step function to cut off the source should not be invoked.

Now an upper bound on the contributions of the three terms can be found by evaluating the first two at $t = R/c$ and the third at $t=R/c +T$ when $T \ll \omega_c^{-1}$. This gives

$$\left(\frac{\delta p}{p}\right)_{max} \approx \frac{e^{z/2H}\,\omega_b \mathcal{F}}{4\pi(\gamma-1)g^2 H\rho} \left\{ \left(-\frac{\omega_c^2}{2c}\right) + (-2V)\left(-\left(\frac{1}{2RH} + \frac{z}{R^3} - \frac{\gamma-1}{2\gamma^2}\frac{z^3}{R^3H^2}\right)\right) + \left(\frac{\omega_c^2\,(\gamma-1)\,z^2}{8\,\gamma^2\,H^2\,R}\,T\right) \right\} \qquad (3\text{-}17)$$

For the parameters considered later for distant observations of a 1 MT sea level burst, it will be found that the second term is the dominant element of the expression.

D.2 Rising Mass Dipole Source

The flow of air around a rising fireball, at points outside the fireball itself, resemble a dipole flow around a moving source pair (source and sink) separated by roughly a fireball diameter. This combination of motion and point sources can easily be simulated to provide an alternate model for the fireball rise mechanism as a gravity wave source. Since it is not clear exactly which aspect of the fireball rise is most important in production of gravity waves, it is best to provide models for several features.

A pair of rising mass sources displaced vertically by a separation Δz and acting over a finite time, T, can be described by

$$Q = \frac{1}{\rho}\frac{dM}{dt}\ \delta(x)\ \delta(y)\ [\delta(z-Vt) - \delta(z-Vt-\Delta z)]\ [\theta(t) - \theta(t-T)] \qquad (3\text{-}18)$$

where the net emission of mass is exactly zero. A single one of the pair of sources emits mass at a rate dM/dt while the other absorbs mass at the same rate. Since the net effect of the motion of the fireball (at constant velocity V) is to move air from above to below the fireball the displaced mass will give

$$\frac{dM}{dt} = \rho\pi a^2 V \qquad (3\text{-}19)$$

where "a" is the fireball radius. We will take dM/dt to be constant and simply treat the density, ρ, as a parameter.

We will now sketch the calculation required for a single source and take the sum of two following the final step. Consider the source

$$Q = \frac{1}{\rho}\frac{dM}{dt}\ \delta(x)\ \delta(y)\ \delta(z-Vt-z_0)\ [\theta(t) - \theta(t-T)] \qquad (3\text{-}20)$$

In the low frequency limit the pressure response to this source is

$$\frac{\delta p}{p} = \frac{e^{z/2H}}{4\pi gH\rho}\,\omega_b\,\frac{dM}{dt}\ \left\{ \int dz'\ \frac{e^{-z'/2H}}{R} \int_{R/c}^{\infty} d\tau J_0\left(\omega_c\,(\tau^2 - R^2/c^2)^{1/2}\right) \cdot \right.$$

$$\cdot\ [\delta(z'-z_0-V(t-\tau))\ (\delta(t-\tau) - \delta(t-\tau-T))$$

$$\left. + \frac{1}{V}\,\delta'\left(t-\tau-\frac{z'-z_0}{V}\right)\ (\theta(t-\tau) - \theta(t-\tau-T))\right] \Bigg\} \qquad (3\text{-}21)$$

After the trivial integrations the result is

$$\frac{\delta p}{p} = \frac{e^{z/2H}\,\omega_b}{4\pi g H \rho}\frac{dM}{dt}\left\{\left.\frac{e^{-z'/2H}}{R}\,J_0\left(\omega_c\,(t^2-R^2/c^2)\right)\right|_{\substack{z'=z_0\\ z'=z_0+VT\\ t=t-T}}\right.$$

$$+\frac{1}{V}\int_{z_0}^{z_0+VT} dz'\,\frac{e^{-z'/2H}}{R}\left[-J_1\left(\omega_c\left((t-\frac{z'-z_0}{V})^2-R^2/c^2\right)\right)^{1/2}\right.$$

$$\left.\left.\cdot\,\omega_c\,\frac{(t-\frac{z'-z_0}{V})}{\sqrt{(t-\frac{z'-z_0}{V})^2-R^2/c^2}}\right]\right\} \qquad (3\text{-}22)$$

If $t < R/c+T$ the first term is evaluated only at $z'=z_0$ and the upper limit of the integral is $z_0+V(t-R/c)$. The peak value of the above expression can be estimated by evaluation of the first term for $t \approx R/c$ and for the second at $t \approx R/c+T$. This gives (for $\omega_c \ll \omega_b$ and $\omega_c T \ll 1$)

$$\left(\frac{\delta p}{p}\right)_{max} \approx \frac{e^{z/2H}\,\omega_b}{4\pi g H \rho}\frac{dM}{dt}\,e^{-z_0/2H}\left(\frac{1}{R}-\frac{\omega_c^2\,T}{2c}\,e^{-VT/2H}\right) \qquad (3\text{-}23)$$

The corresponding result for two sources of opposite sign separated by Δz is then

$$\left(\frac{\delta p}{p}\right)_{max} \approx \frac{e^{(z-z_0)/2H}\,\omega_b}{4\pi g H \rho}\frac{dM}{dt}\left(1-e^{-\Delta z/2H}\right)\left(\frac{1}{R}-\frac{\omega_c^2\,T}{2c}\,e^{-VT/2H}\right) \qquad (3\text{-}24)$$

D.3 Oscillating Sphere

The experimental work by McLaren et al suggests that a buoyant object oscillating about its equilibrium altitude acts as a source of gravity waves. In order to model the contribution of fireball oscillations to gravity wave generation we consider a force source which oscillates in sign and location in such a manner that the associated acceleration is approximately that of a fireball. A damped oscillation can be represented by

$$F_z = A \sin(\omega_0 t)\, e^{-\alpha t}\, \delta(x)\, \delta(y)\, \delta(z - z_0 - \Delta z \sin \omega_0 t)\, \theta(t) \quad (3\text{-}25)$$

where ω_0 is the oscillation frequency and Δz is the amplitude. If a sphere of radius "a" oscillates at a frequency ω_0, the peak acceleration will be $\omega_0^2\, \Delta z$ over a volume of $4\pi a^3/3$. Thus at a density ρ, the net force required to impose such an oscillation will be

$$\mathcal{F} = \omega_0^2\, \Delta z\, 4\pi a^3 \rho/3 = A\rho \quad (3\text{-}26)$$

The pressure fluctuations, in the low frequency limit, can be written as

$$\frac{\delta p}{p} = \frac{e^{\frac{z-z_0}{2H}}\, \omega_b}{4\pi R} \left(\frac{A}{g^2 H\,(\gamma-1)}\right) \int_{R/c}^{\infty} J_0\left(\omega_c \sqrt{\tau^2 - t^2}\right) e^{-\alpha(t-\tau)}$$

$$\cdot \left[\left(-\omega_0^2 \sin(\omega_0(t-\tau)) - 2\alpha\omega_0 \cos \omega_0(t-\tau) + \alpha^2 \sin \omega_0(t-\tau)\right) \theta(t-\tau)\right.$$

$$+ \left(2\omega_0 \cos \omega_0(t-\tau) - 2\alpha \sin \omega_0(t-\tau)\right) \delta(t-\tau)$$

$$\left. + \sin \omega_0(t-\tau)\, \delta'(t-\tau)\right] d\tau \quad (3\text{-}27)$$

Now for distant observation points ω_c is a small compared to α since the fireball motion is damped out after a few oscillations at approximately the Brunt frequency. That is

$$\omega_c \ll \alpha \approx \omega_b/n \tag{3-28}$$

where n is the number of oscillations before damping. As a result the bulk of the time variation of the integral is provided by the exponential factor. This leads to

$$\frac{\delta p}{p} \approx \frac{e^{\frac{z-z_0}{2H}}\ \omega_b\ A}{4\pi\ Rg^2H\ (\gamma-1)} \left\{ \omega_o - (\alpha^2-\omega_o^2)\ \frac{2\pi}{\omega_o^2}\ (-\alpha\ e^{-\alpha(\pi/\omega_o)}) \right\} J_0\ (\omega_c \sqrt{t^2-R^2/c^2}) \tag{3-30}$$

Thus for the above restriction on α, the peak fluctuation will be

$$\left(\frac{\delta p}{p}\right)_{max} \approx \frac{e^{\frac{z-z_0}{2H}}\ \omega_b\ \omega_o^3\ \Delta z\ 4\pi a^3}{12\pi Rg^2H(\gamma-1)} \tag{3-31}$$

D.4 Breathing Sphere

As the fireball bobs vertically about its equilibrium position, it also undergoes expansion and contraction due to the associated variation of ambient pressure. While there is no direct evidence to suggest this is an important gravity wave source, it may be that this mechanism produced the waves seen experimentally by McLaren et al since they could not separate the effects of bobbing and breathing. Therefore we will now give a model for this breathing which is appropriate as a gravity wave source.

The breathing of the fireball can be simulated by an oscillating mass injection which provides no net mass change over a cycle. We will take the mass change to be

$$\Delta M(t) = \Delta M_o \sin(\omega_o t) \tag{3-32}$$

It operates for a single cycle, is continuous and acts at a point. The source for our model is then

$$Q = \frac{\omega_o}{\rho} \Delta M_o \, \delta(\vec{r}) \cos(\omega_o t) \qquad 0 < t < 2\pi/\omega_o \tag{3-33}$$

so the low-frequency response is

$$\frac{\delta p}{p} = -\frac{e^{z/2H} \Delta M_0 \omega_b}{4\pi g H \rho R} \int_{R/c}^{\infty} d\tau \, J_0(\omega_c \sqrt{\tau^2 - R^2/c^2})$$

$$\cdot \left[\omega_o^2 \sin \omega_o(t-\tau) \left[\theta(t-\tau) - \theta(t-\tau-2\pi/\omega_o\right]\right.$$

$$\left. - \omega_o \cos \omega_o(t-\tau) \left[\delta(t-\tau) - \delta(t-\tau - 2\pi/\omega_o)\right]\right] \tag{3-34}$$

The terms in the square bracket have a time scale $\sim \omega_o^{-1}$ while J_0 has a time scale $\sim \omega_c^{-1}$ Consequently, since $\omega_o \approx \omega_b \gg \omega_c$, J_0 can be expanded about $\tau = t$ and the integral can be directly evaluated. When this is done, one finds that the first three terms in the series give no contribution to the integral so that the result is

$$\frac{\delta p}{p} \approx -2\pi \frac{e^{z/2H} \Delta M_0 \omega_b}{4\pi g H \rho R} \cdot \frac{1}{\omega_o^2} \cdot \frac{\partial^3 J_0}{\partial \tau^3} \Bigg|_{\tau=t} \tag{3-35}$$

so the peak value at t = R/c will be

$$\left(\frac{\delta p}{p}\right)_{max} = \frac{e^{z/2H}\,\Delta M_0\,\omega_b}{2gH\rho R\omega_0^2}\left(\frac{\omega_c^6}{48}\left(\frac{R}{c}\right)^3\right) \tag{3-36}$$

E. EFFECTS FROM FIREBALL MOTION MODELS

In order to find the magnitude of the gravity wave response to the fireball motion models presented in subsection D, it is convenient to use a consistent set of parameters appropriate to a typical case of interest. In this we will follow Tolstoy and Lau who considered the example of a one megaton low-altitude explosion as observed at a distant point in the ionosphere.

We will use an observation height of z = 250 km where the density is $\rho \approx 6 \times 10^{-14}$ gm/cm^3. When this is compared to the sea level value ($\rho_0 = 1.2 \times 10^{-3}$), it is seen that a mean scale height of H ≈ 10.5 km is required to provide the proper ratio for an isothermal atmosphere. Fireballs are initially at about 10% ambient density so the density defect is $\beta \approx .9$. For a 1 MT burst the initial fireball radius is a ≈ 1 km. Therefore the fireball rise velocity, for g = 950 cm/s^2, is

$$V \approx \sqrt{ag\beta} \approx 9 \times 10^3 \text{ cm/s} \tag{3-37}$$

The force which must be exerted on a sphere to sustain this motion in a stratified medium is then

$$\mathcal{F}_{max} = \frac{\rho_0 a^4 g}{H} \approx 10^{14} \text{ dynes} \tag{3-38}$$

This is an upper limit since the peak value as a function of velocity has been taken. (Note that this net force is much less than the buoyant force $4/3\pi a^3\rho_0$.) Tolstoy and Lau indicate that the rise time of the fireball before reading its equilibrium altitude is

$$T \approx 300 \text{ sec}$$

This is consistent with experiment by McLaren et al which suggest the rise takes about one Brunt period. In this example

$$\omega_b = \sqrt{\frac{\gamma-1}{\gamma}\frac{g}{H}} = 1.6 \times 10^{-2} \text{ sec}^{-1}$$

so the Brunt period is $\tau_B = 2\pi/\omega_b \approx 390$ seconds. To complete the parameters required we use $\gamma = 1.4$, observation radius of $r = 10^4$km $\approx R$ giving $\omega_c = 4 \times 10^{-4}$ sec^{-1} and $c = 374$ m/s.

Now the rising force model of Equation (3-18) gives

$$\left(\frac{\delta p}{p}\right)_{max} \approx 3 \times 10^{-4} \quad \_ \quad \text{Rising Force}$$

The result for the rising dipole mass source from Equation (3-25) for a separation $\Delta z = 2a$ is

$$\left(\frac{\delta p}{p}\right)_{max} = 4 \times 10^{-3} \quad \_\_ \quad \text{Rising Dipole Mass}$$

The oscillating sphere source provides the result of Equation (3-31) which for an amplitude Δz of 5 km and a frequency of $\omega_o = \omega_b$ gives

$$\left(\frac{\delta p}{p}\right)_{max} = 4 \times 10^{-3} \quad \_\_ \quad \text{Oscillating Sphere}$$

Finally the breathing sphere yields for $\Delta M_0 = 0.1 \cdot 4/3\pi a^3 \rho$, corresponding to a 10% volume fluctuation,

$$\left(\frac{\delta p}{p}\right)_{max} = 2.5 \times 10^{-5} \quad \text{---} \quad \text{Breathing Sphere}$$

For comparison with the blast wave source as provided in Equation (3-14) we take the 1 MT values initialized at $z_0 = 100$ km; $(\delta p/p)_0 = 2.1$ and $T_0 = 100$ seconds. This gives

$$\left(\frac{\delta p}{p}\right)_{max} = 1.5 \quad \text{---} \quad \text{Blast Wave}$$

For comparison with observations it is often useful to express fluctuations in terms of vertical displacement. Generally there is not simple relation between $\delta p/p$ and displacement but in the case of low frequencies a useful result can be given because in this regime the motion is nearly incompressible. Therefore pressure perturbations result from vertical displacements of the neutral air such that

$$\frac{\delta p}{p} \approx \frac{\delta z}{H} \tag{3-39}$$

However observations in the ionosphere are of vertical displacement of the plasma which tends to move with the component of the neutrals along the earth's magnetic field. Furthermore the gravity wave particle motion tends to be radial from the source so that combining this information we find a neutral radial displacement of

$$\delta r \approx \delta z \frac{r}{z} \approx \left(\frac{r}{z}\right) H \frac{\delta p}{p} \tag{3-40}$$

giving a vertical plasma displacement of

$$\Delta z \approx \delta r \sin \theta_d \cos \theta_d \cos \phi \qquad (3\text{-}41)$$

where θ_d is the magnetic dip angle and ϕ is the angle of propagation relative to the magnetic meridian. Thus for typical magnetic angles the product of the trigonometric functions is ~ 1/4. The vertical displacement of the ionospheric plasma from a low frequency pressure fluctuation is then

$$\Delta z \sim \frac{\delta p}{p} \cdot \frac{rH}{4z} \qquad (3\text{-}42)$$

The blast wave calculation for 1 MT as observed at 10,000 km, from previously stated parameters, will be ~ 150 km which is about an order of magnitude greater than that found in the previous section. This difference is largely due to different choices of effective scale heights (10.5 km versus 25 km). Use of 25 km leads to a reduction of about a factor of 30 or to a net Δz of 5 km in the current calculation. This is comparable with the result of Section 2. This illustrates a difficulty of making a direct comparison with experimental results using an isothermal atmosphere model.

F. SUMMARY

The calculations of Section 2 indicate that the gravity waves with periods of up to hours observed at thousands of kilometers from low-altitude large yield nuclear explosions are generated by the blast wave mechanism. In this section we have explored the possibility that the fireball rise and oscillation may also make a significant contribution to gravity waves. To this end a set of four models of fireball motion have been constructed and there effects calculated using the low-frequency theory in conjunction with point sources. It is found that each of the

source models generates only very weak gravity waves relative to the blast wave mechanism giving pressure fluctuations which are about three orders of magnitude less than that from the blast wave source. The models used for fireball motion are rather simple. However in each instance approximations used were chosen to maximize the effects generated. As a result we can be fairly confident that use of more realistic models will not alter the basic result and such calculations are not justified since it seems clear that fireball rise is not a significant source of gravity waves from low altitude nuclear explosions.

SECTION 4
SUMMARY AND CONCLUSIONS

In the present contract DARPA/AFOSR tasked MRC to study the generation of ionospheric gravity waves by nuclear surface bursts to determine what aspects of the explosion are the most important source of ionospheric gravity waves; special consideration has been given to the question of whether or not the traveling ionospheric disturbance observed by Lewis Duncan at Arecibo on 22 September 1979 could have been caused by a small low altitude explosion and to the more general question of whether or not ionospheric gravity waves are likely to be useful for detecting small, low-altitude nuclear explosions at great distances from the burst. We have made the necessary calculations and have obtained good agreement with the data - the first time such agreement has been obtained from a theoretical calculation. The calculated gravity wave signal agrees with observation in magnitude, scales correctly with observation distance(i.e., its period increases linearly with distance, it maximum amplitude decreases as 1/R) and with yield (i.e., its period independent of yield and the amplitude proportional to yield).

In the semiannual report[6] we presented the results of the generation of ionospheric gravity waves by the high altitude hot spot above a low altitude nuclear explosion; that work primarily considered waves traveling in the ducted modes. In the present report we have calculated the generation of gravity waves by the blast wave and by the rising fireball. In this work we have considered isothermal atmospheres and so have only freely propagating modes (the coupling of the blast wave to the ducted gravity modes in a two layer atmosphere was calculated in Reference 7).

On the basis of our research we have reached the following conclusions: 1) the major source of the large amplitude ionospheric gravity wave observed following the U.S. and Soviet tests (the wave with periods ranging from 30 minutes to more than two hours is the blast wave and the energy is transmitted by the freely propagating modes; 2) the source of the 15 minute period wave that were observed to go all the way around the world is the high altitude hot spot and the energy is traveling in the ducted modes; 3) the motions associated with the rising fireball give a smaller signal in the freely propagating modes than the blast wave; 4) it appears that ionospheric observations will be of limited use in detecting small (>10kT) low altitude detonations at large distances (>1000km) from the burst.

REFERENCES

1. Kanellakos, D. P., "Response of the Ionosphere to the Passage of Acoustic - Gravity Waves Generated by Low-Altitude Nuclear Explosions", J. Geophys. Res. 72, 4559, 1967.

2. Anastassiades, M., D. Ilias, G. Moraitis, and P. Giouleas, "Observations Made by the Ionospheric Institute of Athens during the Series of Nuclear Weapons Test of Novaja Zemlya between 10 September and 4 November 1961," AGARD-CP-265 (1963).

3. Tolstoy, I., and T. J. Herron, "Atmospheric Gravity Waves from Nuclear Explosions", J. Atmos. Sci. 27, 55, 1970.

4. Francis, S. H., "Global Propagation of Atmospheric Gravity Waves: A Review," J. Atmos. and Terr. Phys. 37, 1011, 1975; see also "Acoustic Gravity Waves in the Atmosphere," DARPA Conference proceedings, Boulder, 1968.

5. Thome, G. D., "Long Period Wave Generated in Polar Ionosphere During the Onset of Magnetic Storms," J. Geophys. Res. 73, 6319, 1967.

   Hines, C. O., "Atmospheric Gravity Waves; A New Toy for the Theorist", Radio Sci., 690, 375 (1965).

6. Wortman, W. R. and G. D. McCartor, "Ionospheric Gravity Waves from Nuclear Surface Bursts", MRC-R-765, Mission Research Corporation, June 1983.

7. McCartor, G. D., "The Coupling Between Explosively Generated Atmospheric Pulses and Ducted Traveling Ionospheric Disturbances", MRC-R-638, Mission Research Corporation, May 1983.

8. Longmire, C. L., G. D. McCartor and W. R. Wortman, "Ionospheric Effects and Energy Loss from the Blast Wave From Low Altitude Nuclear Bursts", MRC-R-137, Mission Research Corporation, December 1974.

9. Knabe, W. E. and S. L. Kahalas, "Generation of Gravity-Acoustic Waves by Nuclear Detonations," in Acoustic-Gravity Waves in the Atmosphere, ESSA/ARPA, (1968).

10. Pierce, A. D., "A Model for Acoustic-Gravity Wave Excitation by Buoyantly Rising and Oscillating Air Masses," in Effects of Atmospheric Acoustic Gravity Waves on Electromagnetic Wave Propagation, AGARD-CP-115, (1972).

REFERENCES (Concluded)

11. Murphy, B. L. and S. L. Kahalas, "Modeling of Nuclear Sources of Acoustic Gravity Waves," in Effects of Atmospheric Acoustic Gravity Waves on Electromagnetic Wave Propagation, AGARD-CP-115, (1972).

12. Scorer, R. D., "Experiments in Convection of Isolated Masses of Buoyant Fluid," J. Fluid Mech. 2, 583, (1957).

13. Warren, F. W. G., "Wave Resistance to Vertical Motion in a Stratified Fluid," J. Fluid Mech. 7, 209 (1960).

14 Tolstoy, I. and J. Lau, "Generation of Long Internal Gravity Waves in Waveguides by Rising Buoyant Air Masses and Other Sources," Geophys. J. Roy. Astron. Soc. 26, 295 (1971).

15. Mowbray, D. E. and B. S. H. Rarity, "A Theoretical and Experimental Investigation of the Phase Configuration of Internal Waves of Small Amplitude in a Density Stratified Liquid," J. Fluid Mech. 28, 1 (1967).

16. McLaren, T. I., A. D. Pierce, T. Fohl and B. L. Murphy, "An Investigation of Internal Gravity Waves Generated by a Buoyantly Rising Fluid in a Stratified Medium," J. Fluid Mech. 57, 229 (1973).

17. Wortman, W., G. McCartor and G. Baumann, "Ionospheric Disturbances from Underground Tests," Mission Research Corporation, unpublished (1980).

APPENDIX A
TIME INTEGRATION IN THE STATIONARY PHASE

In this appendix we illustrate the failure of the stationary phase in reproducing exactly the relation

$$d = \int dt\ V(t) \tag{A-1}$$

from the stationary phase evaluation of the integrals

$$V = \int d\omega\ F(\omega)\ e^{i(\omega t - kr)} \tag{A-2}$$

$$d = \int d\omega\ \frac{F(\omega)}{i\omega}\ e^{i(\omega t - kr)} \tag{A-3}$$

To illustrate the source of the problem we assume a simple dispersion relation:

$$\omega^2 = m^2 + k^2 c^2 \tag{A-4}$$

Then the stationary point is obtained by solving

$$\frac{\partial \phi}{\partial \omega} = 0 = ct - \frac{\omega}{\sqrt{\omega^2 - m^2}}\, r \quad , \tag{A-5}$$

which gives:

$$\omega_s = \frac{mtc}{\sqrt{t^2 c^2 - r^2}} \quad , \quad tc > r \tag{A-6}$$

and no solution exists for $tc \leq r$.

The stationary phase evalution of the integral requires

$$\left.\frac{\partial^2\phi}{\partial\omega^2}\right|_{\omega = \omega_s} = \frac{m^2 r}{c(\omega^2-m^2)^{3/2}} = \frac{(c^2t^2-r^2)^{3/2}}{mr^2c} \tag{A-7}$$

and

$$k_s = \frac{mr/c}{\sqrt{t^2c^2-r^2}} \tag{A-8}$$

$$\phi_s = m(t^2-r^2/c^2)^{1/2}/c \tag{A-9}$$

The stationary phase approximation then gives:

$$V_s = \left[\frac{(t^2c^2-r^2)^{3/2}}{2mr^2\pi}\right]^{-1/2} F(\omega_s)\, e^{i\phi_s} \tag{A-10}$$

$$d_s = \left[\frac{(t^2c^2-r^2)^{3/2}}{2mr^2\pi}\right]^{-1/2} \frac{F(\omega_s)}{i\omega_s}\, e^{i\phi_s} \tag{A-11}$$

To carry out the comparison further, we now choose the form of the function $F(\omega)$. In particular, we take

$$F(\omega) = \left[\frac{(t^2c^2-r^2)^{3/2}}{2mr^2\pi}\right]^{1/2} c \tag{A-12}$$

Thus

$$V_s = ce^{i\phi_s}, \tag{A-13}$$

$$d_s = \frac{\sqrt{t^2c^2-r^2}}{imt} e^{i\phi_s} \quad . \tag{A-14}$$

To check we evaluate

$$\frac{dd_s}{dt} = ce^{i\phi_s}\left[1+ \frac{r^2}{i\phi_s c^2 t^2}\right] \neq V_s \tag{A-15}$$

The second term in (A-15) is different from zero for all finite times $t>r/c$ and indicates the magnitude of the error. To improve the agreement between $\int V_s dt$ and d_s it is necessary to include higher order corrections to the stationary phase. Though possible, this becomes quickly impractical, in particular for a complicated dispersion relation of the type needed to analyze the gravity waves.

The result of this appendix indicates that the use of stationary phase in the analysis of the gravity waves is somewhat questionable if a detailed behavior of the atmospheric motion is to be derived. Our main hope is that, at best, the stationary phase is capable of providing qualitative information about general trends, maximum displacement and other gross features of the physics following an atmospheric burst. It is interesting to note that at $t^2>>r^2/c^2$.

$$V_s \sim ce^{imt} \quad , \quad d_s \sim \frac{c}{im} e^{imt}$$

and the stationary phase is exact. It therefore seems reasonable to conjecture that the stationary phase becomes exact as $\omega_s t>>kr$ since ω_s approaches a constant at large t and it is possible to satisfy this condition.

APPENDIX B
GRAVITY WAVES IN TWO-LAYER ATMOSPHERE

We now wish to consider the gravity wave response propagating through the freely propagating modes in a two layer atmosphere. We choose, arbitrarily, z=0 as the altitude of the discontinuity. In each layer, the eigenvectors $|\omega,a\rangle$ given in Equation (2-12) are solutions. We denote by $|\omega,a\rangle_1$ the solution in the lower layer and by $|\omega,a\rangle_2$ the solution in the upper layer. For a disturbance originating below z=0, there will be an upwardly propagating wave $|\omega,a\rangle_1$ and a reflected wave $|\omega,-a\rangle_1$ in the lower layer. In the upper layer, only the outwardly propagating wave occurs. Thus the general solution in a two layer atmosphere is:

$$\begin{aligned} |\omega,a\rangle &= A|\omega,a\rangle_1 + B|\omega,-a\rangle_1 \qquad z<0 \\ &= C|\omega,a\rangle_2 \qquad z>0 \end{aligned} \tag{B-1}$$

In terms of the coefficients defined in Section 2, the matching conditions at z=0

$$c_1 a_2|_{z=0^-} = c_2 a_2|_{z=0^+} \tag{B-2}$$

$$(a_1 + \frac{1}{\gamma-1} a_4)/_{z=0^-} = (a_1 + \frac{1}{\gamma-1} a_4)/_{z=0^+} \tag{B-3}$$

imply:

$$A+B=C \tag{B-4}$$

$$AP_1(a_1)+BP_1(-a_1)+\frac{A+B}{\gamma-1}P_4(a_1) = C(P_1(a_2)+\frac{1}{\gamma-1}P_4(a_2)) \tag{B-5}$$

Here a_i is used to denote the wave propagating below (i=1) and above (i=2) z=0, $P_j(\omega,a)$ are defined in Section 2B.

The matching conditions are readily solved for A/C, B/C and we find:

$$A/C = [P_1(a_2)-P_1(-a_1)+\frac{1}{\gamma-1}(P_4(a_2) - P_4(a_1))]/(P_1(a_1)-P_1(-a_1)) \tag{B-6}$$

$$B/C = [P_1(a_2)-P_1(a_1)+\frac{1}{\gamma-1}(P_4(a_2) - P_4(a_1))]/(P_1(a_1)-P_1(-a_1)) \tag{B-7}$$

and the normalization requires

$$|A|^2 + |B|^2 + |C|^2 = 1 \tag{B-8}$$

These coefficients together with (B-1) provide a complete set of states and we can write:

$$|f(t)> = \int d\omega \int da |\omega,a> <\omega,a|f(0)>e^{-i\omega t} \tag{B-9}$$

and we can carry out calculations as in Section 2.